Development of a Low-Cost Integrated Navigation System for USVs

Haakon Ellingsen

Master of Science in Engineering Cybernetics
Submission date: August 2008
Supervisor: Morten Breivik, ITK

Norwegian University of Science and Technology
Department of Engineering Cybernetics

Problem Description

1. Set up and present a progress plan for your thesis work so that the due date can be met.
2. Review state-of-the-art integrated navigation systems for marine applications with respect to criteria such as
   performance and price.
3. Acquire commercial-off-the-shelf GPS and IMU units (e.g., u-blox and MicroStrain products) and co-locate these
   units in a suitable container.
4. Develop sensor fusion algorithms for integration of GPS and IMU signals. Verify and validate your design by
   numerical simulations in Matlab/Simulink.
5. Verify and validate your design by full-scale experiments with a USV.

Assignment given: 14. January 2008
Supervisor: Morten Breivik, ITK

Abstract

This report considers the real-time implementation approach of an integration between an Inertial Navigation System (INS) and a Global Positioning System (GPS). The integration has been performed, using a GlobalSat EM–411 GPS receiver and a Microstrain 3DM–GX1 Inertial Measurement Unit (IMU). This has been performed by incorporating a Kalman filter, and aiding the INS estimates through GPS measurements.

The goal of this thesis is to create an integrated application able to achieve performance of existing solutions three times the cost.

The implementation has been made in real-time in c++, and off-line in Matlab. However the c++ code has not been sufficiently tested due to computer processing problems. Also the code has not been tested on an actual unmanned surface vehicle.

The integrated solution worked sufficently when the GPS was online. However, during GPS droupout, the result is subject to high position drift, resulting in position errors of up to 400 meters after 20 seconds. Although it is unknown quite how large the position deviation of other, existing solutions are. However, high drift during GPS dropouts renders the IMU estimates quite useless for navigation. Thus this experiment has been unsuccessful.

Acknowledgements

I would like to thank my advisor, Morten Breivik for helping me and advising me on the progress of my work and my report.

I'd also like to thank Vegard Evjen Hovstein and the rest of the Maritime Robotics team for giving me access to their analysis of existing solutions and making this work possible by financing the inertial measurement unit. A special thanks to Arild Hepsø for his assistance with Maritime Robotics existing c++ code and incorporating my code into theirs.

Finally I'd like to thank Bjørnar Vik for giving me valuable insight in equations and integration techniques, as well as sharing from his previous hands-on experience.

Contents

List of Figures

List of Tables

Notation and Abbreviations

Notation

x	Standard typing means that x is a scalar
$\mathbf{R}$	Boldfaced typing means that $\mathbf{R}$ is a matrix or vector
$\mathbf{x}$	True value of $\mathbf{x}$
$\hat{\mathbf{x}}$	Estimated value of $\mathbf{x}$
$\bar{\mathbf{x}}$	Measured value of $\mathbf{x}$
$\tilde{\mathbf{x}}$	Denotes the error, $\mathbf{x} - \bar{\mathbf{x}}$
$\mathbf{R}_a^b$	$\mathbf{R}$ is the rotational matrix that transforms a set of vectors from frame a to frame b
$\dot{\mathbf{x}}$	The dot represents time differentialization of $\mathbf{x}$, $\dot{\mathbf{x}} = \frac{d\mathbf{x}}{dt}$
$\boldsymbol{\omega}_{ba}^a$	Rate of angular rotation of frame a with respect to frame b, coordintized in frame a

Variables

$\boldsymbol{\theta}$	Euler angles
$\boldsymbol{\omega}$	Rate of angluar rotation
$\boldsymbol{\alpha}$	Rate of angular acceleration
$\mathbf{p}$	Position vector
$\mathbf{v}$	Velocity vector
$\mathbf{a}$	Acceleration vector
$\boldsymbol{\Omega}$	Skew symmetric form of $\boldsymbol{\omega}$, $\boldsymbol{\Omega} = (\boldsymbol{\omega}\times)$ (cross-product)
u	Longitudinal horizontal speed (surge)
v	Lateral horizontal speed (sway)
w	Vertical speed (heave)
p	Body frame roll rate
q	Body frame pitch rate
r	Body frame yaw rate
ϕ	Roll in Euler angle
θ	Pitch in Euler angle
ψ	Yaw in Euler angle
(Φ, λ)	Latitude, longitude

Abbreviations

CET	–	Circular Error Propable
DGPS	–	Differential GPS
DoD	–	(United States) Department of Defense
DOF	–	Degrees Of Freedom
DoT	–	(United States) Department of Transportation
ECEF	–	Earth Centered, Earth Fixed
FAA	–	(United States) Federal Aviation Administration
GPS	–	Global Positioning System
IMU	–	Inertial Measurement Unit
INS	–	Inertial Navigation System
HDOP	–	Horizontal Dilution Of Precision
L1	–	f_1 GPS carrier frequency
L2	–	f_2 GPS carrier frequency
NED	–	North–East–Down (frame)
NMEA	–	National Marine Electronics Association
NTNU	–	Norwegian University of Science and Technology
RMS	–	Root Mean Square
SA	–	Selective Availability
USV	–	Unmanned Surface Vehicle
UTC	–	Universal Time, Coordinated
VDOP	–	Vertical Dilution Of Precision
WAAS	–	Wide Area Augmentation System
WGS	–	World Geodetic System

Chapter 1

Introduction

1.1 Motivation

Unmanned Surface Vehicles (USV) has been in used in service of the military since World War II, but has not become largely popular until the 1990s. It is still commonly found in military applications, but is also increasingly found in research vessels.

USVs are commonly used to search for underwater mines or underwater activities, investigate the sea bottom, rescue vessels, reconnaissance and surveillance vessels or as a support vehicle for, e.g., an autonomous underwater vehicles.

Unmanned surface vehicles are usually relatively small, often the size of a recreational watercraft (below 15 meters), and so far, a USV exceeding 100 tons has yet to be found [1]. As USVs are usually quite small, they are also somewhat inexpensive compared to larger vessels. Furthermore, as they are autonomous or remotely operated, proper navigation systems are neccesary to be able to implement successful control algorithms. As proper navigation systems usually also has a high price, they are concidered to be unfit for these applications, as they will drastically increase the price of the USV.

1.2 Background

The Global Positioning System (GPS) represents an inexpensive and global method of obtaining the position of a vessel. Although the measurements are highly subjected to noise, the accuracy can be improved by applying the principle of differential GPS. However, the system gives a low bandwith, especially when it comes to acceleration and speed, which can be calculated by differentiating the position measurements.

As a contrast, an Inertial Navigation System (INS) only measures the forces acting on an Inertial Measurement Unit (IMU), and can thus be used to calculate both speed and position estimates without differentiating. In addition to achieving higher bandwiths on the measurements than GPS, this approach gives the estimates the same bandwith as the acceleration measurements[1]. Furthermore, the INS does not rely on external signals and is therefore not susceptible to jamming nor the problem of areas lacking satellite coverage. Using an INS isn't problem free however, as it suffers from problems with drift of speed and position and is also significantly more expensive than GPS equipment.

IMUs are placed on a platform inside/on the vessel, referred to as IMU platform. This will be discussed later in the report.

There are several reasons why an integration of GPS and an INS is desirable. Generally, an INS gives several advantages that the GPS-system lacks, and vice versa. Several sources approaches this problem, e.g., [4], [8], [9] and [11]. The main reasons for performing such an integration is:

- The INS results are available whenever the GPS measurements are unavailable due to, e.g., interference or jamming, and can also be applied to underwater vehichles
- The INS measurements are obtained without significant time delays
- The INS provides acceleration and speed measurements without differentiation, and is thus less susceptible to noise
- Integration provides real time estimates, as opposed to differentation
- The GPS corrects the integration error from a stand-alone INS system
- The GPS allows on-line calibration of IMU errors and alignment of the IMU platform

[1]In other words, by integrating the measurements, position and speed can be obtained at the same bandwith as the measurement unit.

1.2.1 Survey of Existing Solutions

As of this date, several integrated solutions between GPS and INS already exists, but are in general known to be relatively expensive. For use in low cost applications, like for a small Unmanned Surface Vehicle (USV), a commercial, existing integrated solution can easilly exceed the price of the USV itself. Thus, it is desirable to develop a low-cost integrated solution between a GPS and an INS, using low-cost components in order to keep the total cost down. One state-of-the-art integrated navigation system is the Kongsberg

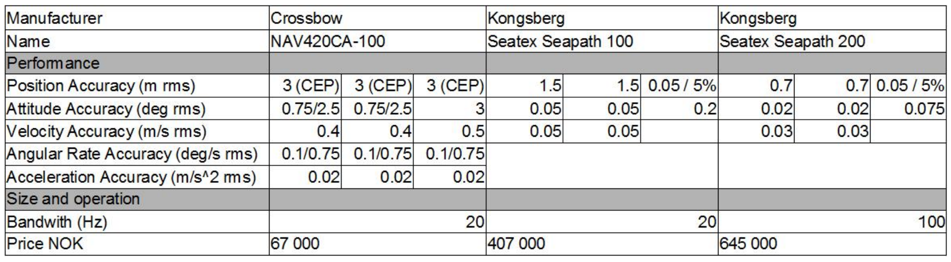

Manufacturer	Crossbow			Kongsberg			Kongsberg		
Name	NAV420CA-100			Seatex Seapath 100			Seatex Seapath 200		
Performance									
Position Accuracy (m rms)	3 (CEP)	3 (CEP)	3 (CEP)	1.5	1.5	0.05 / 5%	0.7	0.7	0.05 / 5%
Attitude Accuracy (deg rms)	0.75/2.5	0.75/2.5	3	0.05	0.05	0.2	0.02	0.02	0.075
Velocity Accuracy (m/s rms)	0.4	0.4	0.5	0.05	0.05		0.03	0.03	
Angular Rate Accuracy (deg/s rms)	0.1/0.75	0.1/0.75	0.1/0.75						
Acceleration Accuracy (m/s^2 rms)	0.02	0.02	0.02						
Size and operation									
Bandwith (Hz)			20			20			100
Price NOK	67 000			407 000			645 000		

Figure 1.1: Statistics of commercial INS/GPS solutions.

Seatex Seapath series. As can be seen from Figure 1.1, both the Seapath 100 and 200 is very expensive, but has very little deviation. The Crossbow NAV420CA–100 is far cheaper, almost $\frac{1}{10}$ of the price of the Seapath 200, but in return has a significantly reduced accuracy. This system is one of the less expensive products on the marked, but still about 3 times the cost of the hardware considered for our purposes. Thus a performance close to the NAV420 will be considered satisfactory.

All the data presented in Figure 1.1 has been obtained from the respective manufacturers by Maritime Robotics. Most data is presented as Root Mean Square (RMS) error, with the exceptance of the position accuracy of the Crossbow solution, which is given in Circular Error Propable (CEP). CEP is a common measure of the accuracy of weapons, giving the radius of a circle whence the projectile will land 50% of the time. Thus the Crossbow will have a position estimate of less than 3 meters 50% of the time.

Despite all efforts, deviation data for solutions when the GPS is disabled has not been obtained. This makes it somewhat difficult to come a definite conclution when comparing two different solutions, as this is one of the key attributes of usch an integrated solution.

An approximate relationship between performance and price is shown in Figure 1.2, beginning at 40 000 NOK. It is unsure whether this will be accurate

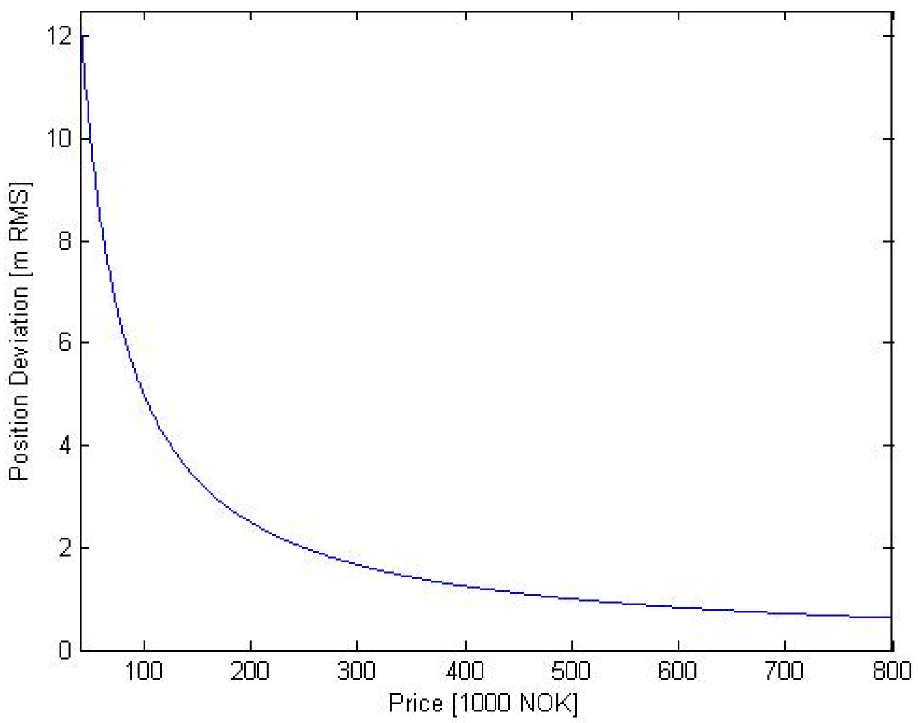

Figure 1.2: Accuracy versus price for commercial INS/GPS solutions.

for prices below 60 000, since RMS position deviation for differential GPS range as low as 3 meters.

1.3 Outline

Chapter 1 discusses the motivation for the assignment and shows data for existing integrated solutions.

Chapter 2 presents different reference frames and different equations used in order to transform a vector from one frame to another.

Chapter 3 looks at the history behind the Global Positioning System and inertial navigation. It also discusses potential errors they are suspectible to and gives equations for estimating position and speed based on acceleration measurements.

Chapter 4 outlines the system equations used for integrating the two navigational systems and the approach to estimate attitude, velocity and acceleration.

Chapter 5 shows the results of the integration and compares them with properties from existing solutions

Chapter 6 concludes the report, and also contains a discussion regarding the concidered product and future work.

Chapter 2

Reference Frames and Transformations

2.1 Reference Frames

In navigation, several reference frames can be used to present the data. Depending on what navigational system is used to obtain the measurements, different reference systems are usually required.

2.1.1 Inertial Frame

For the inertial frame, Newton's law's of motion applies. This means that the frame itself can not accelerate, but is either stationary or travels with constant speed. Its origin can be chosen anywhere.

2.1.2 Earth Centered – Earth Fixed

The Earth Centered, Earth Fixed (ECEF) frame has, as the name suggests, its center in the center of the Earth, and the frame is stationary relative to the surface. Of all the possible combinations of ECEF coordinate systems, two are of particular importance.

The first representation frame gives its position in cartesian coordinates, based on its distance from the center according to each axis. This is named the ECEF rectangular system but is usually just referred to as the ECEF

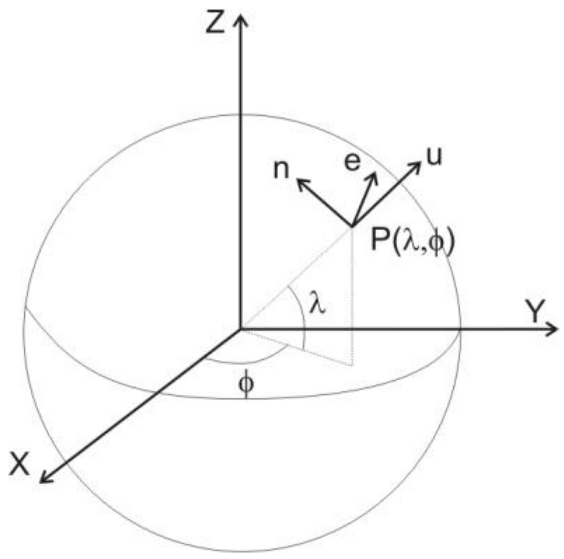

Figure 2.1: The Earth with both ECEF frames and the local geodetic frame.

system. Its x-axis points through the intersection of the prime median (0° longitude), and equator (0° latitude), its z-axis towards the true north pole, and the y-axis to complete the right hand rule through the intersection of 90° longitude and equator.

The other representation is called ECEF geodetic frame. This system expresses position in latitude, longitude and height, $[\Phi, \lambda, h]$ and is given in the spherical coordinates. The system takes its basis in the ECEF rectangular frame. The latitude is found by rotating around the z-axis until the x-axis crosses the projection from the position on to the x-y-plane. The longitude is then found by rotating around the y-axis until the x-axis coincides with the vector from the center of the Earth to the position. The height is the distance from the nearest point normal on the assumed altitude.

The altitude is assumed to be at the surface of the WGS-84 ellipsoid. WGS-84, or the World Geodetic System, is an estimate of Earth dating back to 1984. This ellipsiod will be concidered furter upon developing a gravity model in Section 3.1.6.

Both ECEF frames are depicted in Figure 2.1, as well as the ENU-frame, which will be presented later.

Geographic Frame

The geographic frame is dependent on its origin and is only locally correct. It is earth fixed and has its origin at the ellipsoid used to describe the surface of the Earth. The x-axis points north, the y-axis towards east and the z-axis points down, normal onto the ellipsoid.

Geosentric Frame

This frame is equal to the geographic frame, with the difference that its z-axis is pointing towards the center of the Earth.

2.1.3 Local Geodetic or Tangent Plane

The local geodetic frame is the frame most people consider when orienting themselves. It takes basis of making a fictional tangent plane at the origin, just like presenting the globe as a map. The x-axis points north, the y-axis towards east and the z-axis points down, normal onto the ellipsoid, therefore also widely known as the NED-frame (north-east-down). This frame coincides with the geographic frame for a stationary target. The difference between the two is that in the latter frame, the origin is a projection of the platform origin onto the Earth's geoid.

Another version of this frame is the east, north, up-frame (ENU).

2.1.4 Body Frame

In the body frame, the origin is usually in the center of gravity of the body of the object in question. Its x-axis points towards the defined front of the object, the z-axis points down and the y-axis points right to complete the right hand rule. This frame is, together with the NED-frame, widely used for control purposes.

The frame represents the vessel states in 6 degrees of freedom (6 DOF) known as surge, sway and heave (u, v, w), and roll, pitch and yaw (ϕ, θ, ψ). Surge, sway and heave is the speed in x, y and z respectively, and roll, pitch and yaw is the vehicle's angular displacement from the NED-frame.

2.2 Rotation Matrices and Transformations

In order to transform states from one frame to another, rotation matrices can be used. For a rotation matrix, subscripted letters indicate the frame it is being transformed *from*, while superscripted letters denote the frame the states are being transformed *to*. Thus,

$$\mathbf{R}_p^b$$

means the states are transformed from the platform to the body frame.

2.2.1 ECEF Geodetic to ECEF Rectangular

The geodetic coordinates, given in latitude and longitude, (Φ, λ) only gives coordinates in two directions, namely north and east. The height is then assumed zero, unless stated otherwise, according to the ellipsoid model of the Earth's geoid being used. In particular, the WGS-84 ellipsoid is commonly used. As already stated, the model parameters will be considered further when discussing the gravity model in Section 3.1.6, but for now only a few parameters is of importance.

The ellipsoid has two constants needed to define the model. These are the semimajor and semiminor axis, noted as a and b respectively. The semimajor axis is the longest of the two, going horizontally from the center of the Earth, along the xy-plane in Figure 2.1. The semiminor axis is thus the one pointing vertically along the z-axis. The length of the semimajor axis is

$$a = 6378137.0,$$

while the semiminor axis is only needed to calculate the flatness of the ellipsoid, defined as

$$f = \frac{a-b}{a} = \frac{1}{298.257223563}.$$

Since [15] already has provided f, an explicit value of b is not needed. Furthermore, the eccentricity of the ellipsoid is defined as

$$e = \sqrt{f(2-f)} = 8.1819190842622 \cdot 10^{-2}.$$

Finally, the length of the normal of the ellipsoid, from the surface of the ellipsoid to the intersection with the ECEF z-axis is given as

$$N(\phi) = \frac{a}{\sqrt{1 - e^2 sin(\Phi)^2}}, \tag{2.1}$$

which is used for the transformation between the two frames. To calculate rectangular coordinates,

$$x = (N + h)cos(\Phi)cos(\lambda) \tag{2.2}$$

$$y = (N + h)cos(\Phi)sin(\lambda) \tag{2.3}$$

$$z = [N(1 - e^2) + h]sin(\Phi) \tag{2.4}$$

The transformation the other way around is a bit trickier, and is not very relevant for this report. It will thus not be discussed here.

2.2.2 ECEF-to-Tangent-Plane Transformation

The transformation from ECEF- to tangent-plane coordinates, starts by subtracting the tangent-plane origin, given in the ECEF-frame, from the ECEF coordinates,

$$\delta\mathbf{x} = (x, y, z)^T - (x_0, y_0, z_0)^T, \tag{2.5}$$

leaving the two planes with the same origin. The next step is performing a rotation around the ECEF z-axis until the y-axis is aligned with tangent-plane east:

$$\mathbf{R}_1 = \begin{bmatrix} cos(\lambda) & sin(\lambda) & 0 \\ -sin(\lambda) & cos(\lambda) & 0 \\ 0 & 0 & 1 \end{bmatrix}, \tag{2.6}$$

where λ is the longitude.

By performing a new rotation, this time around the aligned y-axis until the new z-axis is aligned with the tangent-plane down:

$$\begin{aligned} \mathbf{R}_2 &= \begin{bmatrix} cos(\Phi + \frac{\pi}{2}) & 0 & sin(\Phi + \frac{\pi}{2}) \\ 0 & 1 & 0 \\ -sin(\Phi + \frac{\pi}{2}) & 0 & cos(\Phi + \frac{\pi}{2}) \end{bmatrix} \\ &= \begin{bmatrix} -sin(\Phi) & 0 & cos(\Phi) \\ 0 & 1 & 0 \\ -cos(\Phi) & 0 & -sin(\Phi) \end{bmatrix}, \end{aligned} \tag{2.7}$$

where ϕ is the latitude. Please note that this notation is opposite than that of [9], as the notation used in this report is believed to be more commonly used. By combining the two, the complete rotation matrix is obtained,

$$\mathbf{R}_E^t = \begin{bmatrix} -sin(\Phi)cos(\lambda) & -sin(\Phi)sin(\lambda) & cos(\Phi) \\ -sin(\lambda) & cos(\lambda) & 0 \\ -cos(\Phi)cos(\lambda) & -cos(\Phi)sin(\lambda) & -sin(\Phi) \end{bmatrix}. \tag{2.8}$$

2.2.3 Body-to-Tangent-Plane Transformation

This transformation is performed by using the Euler angles derived from the body frame and transforming via one axis at a time. By chosing to start with the rotation around the z-axis the new coordinates $\begin{bmatrix} x' & y' & z' \end{bmatrix}^T$ is obtained

$$\begin{bmatrix} x' \\ y' \\ z' \end{bmatrix} = \begin{bmatrix} cos(\psi) & sin(\psi) & 0 \\ -sin(\psi) & cos(\psi) & 0 \\ 0 & 0 & 1 \end{bmatrix} \begin{bmatrix} x \\ y \\ z \end{bmatrix}. \tag{2.9}$$

The same method is applied to the two remaining axes

$$\begin{bmatrix} x'' \\ y'' \\ z'' \end{bmatrix} = \begin{bmatrix} cos(\theta) & 0 & -sin(\theta) \\ 0 & 1 & 0 \\ sin(\theta) & 0 & cos(\theta) \end{bmatrix} \begin{bmatrix} x' \\ y' \\ z' \end{bmatrix} \tag{2.10}$$

$$\begin{bmatrix} u \\ v \\ w \end{bmatrix} = \begin{bmatrix} 1 & 0 & 0 \\ 0 & cos(\phi) & sin(\phi) \\ 0 & -sin(\phi) & cos(\phi) \end{bmatrix} \begin{bmatrix} x'' \\ y'' \\ z'' \end{bmatrix}, \tag{2.11}$$

and thus having obtained the body frame coordinates. These can be combined by multiplication, yielding

$$\mathbf{v}^b = \begin{bmatrix} cos(\psi) & sin(\psi) & 0 \\ -sin(\psi) & cos(\psi) & 0 \\ 0 & 0 & 1 \end{bmatrix} \begin{bmatrix} cos(\theta) & 0 & -sin(\theta) \\ 0 & 1 & 0 \\ sin(\theta) & 0 & cos(\theta) \end{bmatrix} \begin{bmatrix} 1 & 0 & 0 \\ 0 & cos(\phi) & sin(\phi) \\ 0 & -sin(\phi) & cos(\phi) \end{bmatrix} \mathbf{v}^t$$

$$= \begin{bmatrix} cos(\psi)cos(\theta) & sin(\psi)cos(\theta) & -sin(\theta) \\ -sin(\psi)cos(\theta) + cos(\psi)sin(\theta)sin(\phi) & cos(\psi)cos(\phi) + sin(\psi)sin(\theta)sin(\phi) & cos(\theta)sin(\phi) \\ sin(\psi)sin(\phi) + cos(\psi)sin(\theta)cos(\phi) & -cos(\psi)sin(\phi) + sin(\psi)sin(\theta)cos(\phi) & cos(\theta)cos(\phi) \end{bmatrix} \mathbf{v}^t$$

$$= \mathbf{R}_t^b \mathbf{v}^t \tag{2.12}$$

2.2.4 Platform-to-Body Transformation

Assume a rigidly attached point on the vessel where the measurement sensors are placed. The center of this platform is usually chosen as the origin of the platform frame. As the placement of this platform will differ from each vessel, no standard transformation can be performed. For inertial sensors the platform is adviced to be placed near the center of inertia of the vessel while stationary relative to Earth[1].

[1]The center of inertia will shift whenever in motion, particularly for maritime vessels.

First, assume the IMU being placed at the center of inertia, but with angles relative to the body frame noted as $[\phi_r, \theta_r, \psi_r]$. The rotation to the body frame is then performed by multiplying with (2.12), substituting the respective angles with the ones relative to the body frame. Rotation to the tangent-plane can be performed by adding the body-frame Euler angles to the relative angles.

Second, should the platform be positioned elsewhere, the first step is needed to align the axis. Assume $\mathbf{r}^b$ is a vector denoting the correct displacement from the center, given in body-frame coordinates. As the IMU will detect accelerations of the given point, regardless of position relative to the object it is placed on, the position can be calculated as usual, and the position displacement subtracted from the position,

$$\mathbf{p}^b = \mathbf{R}_p^b \mathbf{p}^p + \mathbf{r}^b. \tag{2.13}$$

For speed and accelerations, the equation needs to be differentiated. First, considering speed,

$$\begin{aligned} \mathbf{v}^b = \dot{\mathbf{p}}^b &= \frac{d}{dt}[\mathbf{R}_p^b \mathbf{p}^p + \mathbf{r}^{\mathbf{b}}] && (2.14) \\ &= \mathbf{R}_p^b \mathbf{v}^p + \dot{\mathbf{R}}_p^b \mathbf{p}^p && (2.15) \end{aligned}$$

Since the rotation matrix is constant, its derivative is equal to zero. The same can be done for the acceleration, yielding

$$\begin{aligned} \mathbf{a}^b &= \mathbf{R}_p^b \mathbf{a}^p && (2.16) \\ \mathbf{v}^b &= \mathbf{R}_p^b \mathbf{v}^p && (2.17) \end{aligned}$$

Chapter 3

System Consept

3.1 Inertial Measurement Units

As opposed to the GPS, which relies on external synchronization to achieve an estimate of the position, an Inertial Navigation System measures acceleration using the physical laws of nature. A pure INS consists only of accelerometers and gyros, and is based on the principle that estimates of the position and velocity is obtained by integrating the acceleration.

When reffering to Inertial Measurement Units, it is assumed to consist of a total of three accelerometers and three gyros. Proper IMUs are generally very expensive, due to need for very accurate measurements. The reason why accurate measurents are needed, is that the acceleration is integrated twice to obtain the position. Any error in the acceleration measurement will also be integrated, and cause a bias on the estimated velocity and a continous drift on the position estimate, unless corrected. Correcting this error is impossible on a pure INS', unless recalibrated or reset.

An INS is commonly aided by magnetometers, being able to detect attitude, and GPS to measure position. For aviation applications, hydroaltimeters are common to detect altitude. As a single GPS receiver is unable to detect drift in attitude, it relies on external aiding to correct the error, through, e.g., GPS compass[1] or magnetometer.

Originally, INS was developed for missiles, but is today also commonly found in airplanes, submarines, spacecraft and ships.

[1]Two or more GPS receivers placed on two previously known locations, used to estimate the heading or other Euler angles.

3.1.1 Accelerometers

An ideal accelerometer can be viewed as an ideal mass spring damper system, where the position, $\mathbf{p}$, relative to the casing is assumed perfectly measured [9]. Then

$$\ddot{\mathbf{p}} = -\frac{k}{m}\mathbf{p} - \frac{b}{m}\dot{\mathbf{p}}, \tag{3.1}$$

where k is the spring constant, b is the damping constant and m is the mass. $\delta\mathbf{p}$ denotes the positional displacement from the equilibrium. The force measured from the accelerometers is defined as

$$\mathbf{f} = \ddot{\mathbf{p}}. \tag{3.2}$$

Should the system also be affected by gravity, the equation becomes

$$\ddot{\mathbf{p}} = -\frac{k}{m}\mathbf{p} - \frac{b}{m}\dot{\mathbf{p}} + \mathbf{g}(\mathbf{p}), \tag{3.3}$$

where $\mathbf{g}(\mathbf{p})$ denotes the position-relative gravity. By comparing with (3.1) and (3.2), it is trivial to see that

$$\mathbf{f} = \ddot{\mathbf{p}} - \mathbf{g}(\mathbf{p}). \tag{3.4}$$

In the case of the accelerometers being within the earth's field of gravity and rotating around the earth's rate of rotation, i.e., resting on the surface of the earth, the equation is adjusted into

$$0 = -\frac{k}{m}\delta\mathbf{p} - \frac{b}{m}\delta\dot{\mathbf{p}} + \mathbf{g}(\mathbf{p}) - \mathbf{\Omega}_{ie}\mathbf{\Omega}_{ie}\mathbf{p}, \tag{3.5}$$

where $\mathbf{\Omega}_{ie}$ is the skew symmetric form of the earth's rate of rotation vector[2]. This equation shows that in case of the accelerometer being stationary relative to the earth's surface, $\mathbf{f} = -\mathbf{g} + \mathbf{\Omega}_{ie}\mathbf{\Omega}_{ie}\mathbf{p}$. When operating in free fall[3], the accelerometers will read 0. This means that the user needs to compensate for the forces of gravity when operating an accelerometer. For the future, the local gravity vector, $\mathbf{g}$, will be defined as **-f**, or

$$\mathbf{g} = \mathbf{g}(\mathbf{p}) - \mathbf{\Omega}_{ie}\mathbf{\Omega}_{ie}\mathbf{p}. \tag{3.6}$$

The INS measures the forces in its current position, denoted as $\mathbf{f}^a$, which has the following properties

$$\mathbf{f}^p = \mathbf{R}_a^p\mathbf{f}^a, \tag{3.7}$$

[2]The equivalent of $\mathrm{S}(\boldsymbol{\omega}_{ie}^i)$ or $(\boldsymbol{\omega}_{ie}^i\times)$

[3]Assuming no rotation.

where

$$\mathbf{R}_a^p \triangleq \begin{bmatrix} 1 & -a_{uw} & a_{uv} \\ a_{vw} & 1 & -a_{vu} \\ -a_{wv} & a_{wu} & 1 \end{bmatrix} \tag{3.8}$$

represents the accelerometer displacement where a_{uw} is to be read as the positive rotation angle about platform w-axis from the uw-plane to accelerometer u-axis.

3.1.2 System Equations

The system can be put on first order form,

$$\dot{\mathbf{p}} = \mathbf{v}^n \tag{3.9}$$
$$\dot{\mathbf{v}} = \mathbf{a}^n. \tag{3.10}$$

Furthermore, the theorem of Coriolis [9] gives

$$\dot{\mathbf{R}}_a^b = \mathbf{R}_a^b \mathbf{\Omega}_{ba}^a. \tag{3.11}$$

(3.10) can be rewritten as

$$\mathbf{M}\dot{\mathbf{v}}^n = \mathbf{f}^n - \mathbf{g}^n = \mathbf{R}_p^n \mathbf{f}^p - \mathbf{g}^n, \tag{3.12}$$

where $\mathbf{g}^n$ is the gravity vector, and $\mathbf{f}$ is the total force acting on the system.

3.1.3 Velocity Dynamics

Inertial Frame

The differential equation for the position vector in an inertial frame is given in (3.4),

$$\ddot{\mathbf{p}} = \mathbf{f} + \mathbf{G}(\mathbf{p}). \tag{3.13}$$

As previously stated, this measurementcan be integrated once to obtain inertial speed, and twice for inertial position. The force in a given inertial frame can be written as a rotation from the body frame,

$$\mathbf{f}^i = \mathbf{R}_b^i \mathbf{f}^b, \tag{3.14}$$

where $\mathbf{R}_b^i$ is the rotation matrix from the body frame to the inertial frame. This can be used to find the differential equation for the rotation matrix in accordance with the theorem of Coriolis stated in (3.11):

$$\dot{\mathbf{R}}_b^i = \mathbf{R}_b^i \mathbf{\Omega}_{ib}^b, \tag{3.15}$$

where

$$\mathbf{\Omega}^b_{ib} \triangleq \begin{bmatrix} 0 & -r & q \\ r & 0 & -p \\ -q & p & 0 \end{bmatrix},$$

i.e., $\mathbf{\Omega}^b_{ib}$ is the skew symmetric form of $\boldsymbol{\omega}^b_{ib} =^{\triangle} [p, q, r]^T$.

This differential equation is more straight-forward than when using any other reference frame. However, it is not very commonly used, due to the difficulty in calculating the gravity $\mathbf{G}(\mathbf{R})$.

Inertial Position, Earth-Relative Velocity

This representation of variables is not very commonly used, as they are impractical to work with. However, it is useful as a means to derive the differential equations of other, more common representations, and is therefore of importance. Here, $\mathbf{p}$ is defined as the position vector relative to the center of earth, and for simplicity, the inertial and ECEF orgins are coincident the center of the earth.

$$\mathbf{p}^e = \mathbf{R}^e_i \mathbf{p}^i. \tag{3.16}$$

Furthermore, the differentiated earth-relative position is the same as the earth-relative speed, $\dot{\mathbf{p}}^e = \mathbf{v}_e$. By using the theorem of Coriolis, this relationship can be written as

$$\frac{d}{dt}\mathbf{p}^i = \mathbf{v}^i + \mathbf{\Omega}^i_{ie}\mathbf{p}^i, \tag{3.17}$$

which is differentiated into

$$\begin{aligned} \frac{d^2}{dt^2}\mathbf{p}^i &= \frac{d}{dt}\mathbf{v}^i + \frac{d}{dt}\mathbf{\Omega}^i_{ie}\mathbf{p}^i \\ &= \frac{d}{dt}\mathbf{v}^i + (\frac{d}{dt}\mathbf{\Omega}^i_{ie})\mathbf{p}^i + \mathbf{\Omega}^i_{ie}\frac{d}{dt}\mathbf{p}^i \\ &= \frac{d}{dt}\mathbf{v}^i + \mathbf{\Omega}^i_{ie}(\mathbf{v}^i + \mathbf{\Omega}^i_{ie}\mathbf{p}^i) \\ \frac{d}{dt}\mathbf{v}^i &= \frac{d^2}{dt^2}\mathbf{p}^i - \mathbf{\Omega}^i_{ie}\mathbf{\Omega}^i_{ie}\mathbf{p}^i - \mathbf{\Omega}^i_{ie}\mathbf{v}^i. \end{aligned} \tag{3.18}$$

In this equation, $\frac{d^2}{dt^2}\mathbf{p}^i$ represents inertial acceleration, $-\mathbf{\Omega}^i_{ie}\mathbf{\Omega}^i_{ie}\mathbf{p}^i$ is the local centrifugal acceleration, while $\mathbf{\Omega}^i_{ie}\mathbf{v}^i_e$ denotes the Coriolis acceleration. The centrifugal acceleration is the same as the gravity, resulting in

$$\frac{d}{dt}\mathbf{v}^i = \mathbf{f}^i + \mathbf{g}^i - \mathbf{\Omega}^i_{ie}\mathbf{v}^i, \tag{3.19}$$

where the calculation of $\mathbf{f}^i$ is shown in (3.13) – (3.15).

ECEF

Since the GPS estimates of the position usually are given in the ECEF frame, it can be convinient to also present the inertial measurements using the same coordinates. One drawback with using this conversion is the complicated gravity calculations.

The position $\mathbf{p}$ and the earth-relative velocity, $\mathbf{v}$, is given as

$$\mathbf{p}^e = \mathbf{R}_i^e \mathbf{p}^i \tag{3.20}$$

$$\mathbf{v}^e = \mathbf{R}_i^e \mathbf{v}^i. \tag{3.21}$$

The relative velocity is given as in the previous example. The differential equation is given by applying the theorem of Coriolis,

$$\dot{\mathbf{v}}^e = \mathbf{R}_i^e (\dot{\mathbf{v}}^i - \mathbf{\Omega}_{ie}^i \mathbf{v}^i). \tag{3.22}$$

By inserting 3.19 into 3.22, the complete expression is obtained.

$$\begin{aligned} \dot{\mathbf{v}}^e &= \mathbf{R}_i^e (\mathbf{f}^i + \mathbf{g}^i - 2\mathbf{\Omega}_{ie}^i \mathbf{v}^i) \\ &= \mathbf{f}^e + \mathbf{g}^e - 2\mathbf{\Omega}_{ie}^e \mathbf{v}^e. \end{aligned} \tag{3.23}$$

The specific force in ECEF coordinates is given as

$$\mathbf{f}^e = \mathbf{R}_b^e \mathbf{f}^b, \tag{3.24}$$

where $\dot{\mathbf{R}}_b^e = \mathbf{R}_b^e \mathbf{\Omega}_{eb}^b$ is valid, using $\boldsymbol{\omega}_{eb}^b = \boldsymbol{\omega}_{ib}^b - \mathbf{R}_e^b \boldsymbol{\omega}_{ie}^e$.

Local Geodetic

Local geodetic coordinates are the most trivial coordinates for most people, and corresponds with the coordinates most commonly used in daily life. The frame is also known as the NED frame, since the coordinates are the same as north, east and down. Furthermore, the coordinates are fairly easy to convert from GPS coordinates, and are also practical with regard to control purposes.

The geodetic velocity is related to the inertial velocity through

$$\mathbf{v}^n = \mathbf{R}_i^n \mathbf{v}^i. \tag{3.25}$$

and is differentiated using the theorem of Coriolis

$$\dot{\mathbf{v}}^n = \mathbf{R}_i^n (\mathbf{\Omega}_{ni}^i \mathbf{v}^i + \dot{\mathbf{v}}^i). \tag{3.26}$$

By inserting (3.19), the result yields

$$\begin{aligned}\dot{\mathbf{v}}^n &= \mathbf{R}_i^n(\mathbf{\Omega}_{ni}^i \mathbf{v}^i + \mathbf{f}^i + \mathbf{g}^i - \mathbf{\Omega}_{ie}^i \mathbf{v}^i) \\ &= \mathbf{f}^n + \mathbf{g}^n + (\mathbf{\Omega}_{ni}^n - \mathbf{\Omega}_{ie}^n)\mathbf{v}^n \\ &= \mathbf{f}^n + \mathbf{g}^n + (\mathbf{\Omega}_{ne} - 2\mathbf{\Omega}_{ie}^n)\mathbf{v}^n, \end{aligned} \tag{3.27}$$

where $\mathbf{\Omega}_{ni} = \mathbf{\Omega}_{ne} - \mathbf{\Omega}_{ie}$, giving the specific force as

$$\mathbf{f}^n = \mathbf{R}_b^n \mathbf{f}^b, \tag{3.28}$$

and $\dot{\mathbf{R}}_b^n = \mathbf{R}_b^n \mathbf{\Omega}_{nb}^b$ are valid, using

$$\mathbf{\Omega}_{nb}^b = \mathbf{\Omega}_{ib}^b - \mathbf{R}_n^b(\mathbf{\Omega}_{ie}^n + \mathbf{\Omega}_{en}^n), \tag{3.29}$$

where $\boldsymbol{\omega}_{ib}^b$ is measured by the gyros, $\boldsymbol{\omega}_{ie}^n = \boldsymbol{\omega}_{ie}[cos(\Phi), 0, -sin(\Phi)]$ is the rate of inertial rotation of Earth, and $\boldsymbol{\omega}_{en}^n$ is the transport rate of the navigation frame relative to earth.

3.1.4 Position Dynamics

By assuming the velocity vector has been found, like in the previous section, the position can be found by integrating,

$$\mathbf{p}(t) = \int_0^t \mathbf{v}(\tau)d\tau + \mathbf{p}(0), \tag{3.30}$$

where $\mathbf{p}(0)$ is the initial position.

To obtain geodetic position from tangent plane velocity coordinates, the following differential equation can be used

$$\begin{bmatrix} \dot{\Phi} \\ \dot{\lambda} \\ \dot{h} \end{bmatrix} = \begin{bmatrix} \frac{1}{R_\Phi + h} & 0 & 0 \\ 0 & \frac{1}{(R_\lambda + h)cos(\lambda)} & 0 \\ 0 & 0 & -1 \end{bmatrix} \begin{bmatrix} v_N \\ v_E \\ v_D \end{bmatrix}, \tag{3.31}$$

where R_λ is the radius of curvature in a meridian at a given latitude, and R_ϕ is the transverse radius of curvature,

$$R_\Phi = \frac{a(1-e^2)}{\sqrt{1-e^2 sin^2(\Phi)}^3} \tag{3.32}$$

$$R_\lambda = \frac{a}{\sqrt{1-e^2 sin^2(\Phi)}}, \tag{3.33}$$

a being the radius at equator, and e being the eccentricity.

3.1.5 Gyros

The equations obtained in the previous section applies for both strap-down and stabilized platform systems. The difference between the two lies in the stabilized being actuated to maintain its alignment with a given reference system, while the strap-down system is, as its name suggests, rigidly attached to the body of the vessel.

Mathematically, the difference lies in the rotation matrix, $\mathbf{R}_p^n$. The strap-down system is the easiest to implement[4], and is also the one being implemented in this report, and is therefore considered. Regardless, both systems requires information of the rotational vector

$$\boldsymbol{\omega}_{np}^p = \boldsymbol{\omega}_{ip}^p - \boldsymbol{\omega}_{in}^p. \tag{3.34}$$

The gyros experience $\boldsymbol{\omega}_{ip}^p$ and $\boldsymbol{\omega}_{in}^p = \mathbf{R}_n^p \boldsymbol{\omega}_{in}^n$. For tangent-plane navigation,

$$\boldsymbol{\omega}_{in}^n = \begin{bmatrix} (\dot{\lambda} + \omega_{ie})cos(\Phi) \\ \dot{\Phi} \\ -(\dot{\lambda} + \omega_i e)sin(\Phi) \end{bmatrix} = \omega_{ie} \begin{bmatrix} cos(Phi) \\ 0 \\ -sin(\Phi) \end{bmatrix} + \begin{bmatrix} \frac{v_E}{R_\lambda + h} \\ \frac{-v_N}{R_\Phi + h} \\ \frac{-v_E tan(\Phi)}{R_\lambda + h} \end{bmatrix} \tag{3.35}$$

is valid. For obtaining the attitude,

$$\begin{bmatrix} \dot{\phi} \\ \dot{\theta} \\ \dot{\psi} \end{bmatrix} = \begin{bmatrix} 1 & sin(\phi)tan(\theta) & cos(\phi)tan(\theta) \\ 0 & cos(\phi) & -sin(\phi) \\ 0 & \frac{sin(\phi)}{cos(\theta)} & \frac{cos(\phi)}{cos(\theta)} \end{bmatrix} \begin{bmatrix} p \\ q \\ r \end{bmatrix} \tag{3.36}$$

can be used.

3.1.6 Gravity Model

For use in a geographic reference system, the gravity is calculated based on the WGS-84 ellipsoid model [15]. The vector is defined as

$$\mathbf{g}^n \triangleq \begin{bmatrix} 0 \\ 0 \\ \gamma(\Phi, h) \end{bmatrix} + \begin{bmatrix} \zeta_g \\ -\eta_g \\ \delta_g \end{bmatrix}, \tag{3.37}$$

[4]With regard to hardware.

Constant	Value
a	6378137.0 [m]
f	$\frac{1}{298.257223563}$
e	$8.1819190842622 \cdot 10^{-2}$
γ_a	9.78049000 [m/s^2]
ω	$7292115.0 \cdot 10^{-11}$ [rad/s]
m	0.00344978650684
f_2	$-f + \frac{5}{2}m + \frac{1}{2}f^2 - \frac{26}{7}fm + \frac{15}{4}m^2$
f_4	$-\frac{1}{2} + \frac{5}{2}fm$

Table 3.1: WGS-84 ellipsoid properties [15].

with

$$\gamma(\Phi) = \gamma_a \left[1 + (f_2 + f_4) sin^2(\lambda) - \frac{1}{4} f_4 sin^2(2\Phi) \right] \tag{3.38}$$

$$\gamma(\Phi, h) = \gamma(\Phi) - \frac{2\gamma_h}{2} \left[1 + f + m + (-3f + \frac{5}{2}m) sin^2(\Phi) \right] h + \frac{3\gamma_a}{a^2} h^2. \tag{3.39}$$

The parameter values for the gravity model are given in Table 3.1. For maritime applications, (3.39) is not considered, since the height is close to constant at $h = 0$.

3.2 Global Positioning System

When talking about the Global Positioning System (GPS), people usually refer to the NAVSTAR GPS, which was originally developed by the United States Department of Defense for use in military applications [13].

In 1983, a Korean airliner was shot down by the Soviet air force. Since the disaster could have been avoided with access to a proper navigation system, Ronald Reagan decided to open the NAVSTAR project for the public. GPS has since then become very popular due to its low cost, availability and accuracy.

Russia also has a similar global positioning system, called the GLONASS, and the European Union's Galileo is to be completed around 2011. In addition, China's regional satellite system, Beidou, has been proposed extended to a global system called COMPASS. Some GPS receivers make use of both GLONASS and NAVSTAR data to increase accuracy.

GPS can be divided into space, control and user segments [9]:

- The space segment is the satellites orbiting the earth. It consists of six planes with four satellites on each plane for a total of 24 satellites. These planes are arranged in such a way that gives at least six satellites line of sight to almost any given point at all times.
- The control segment monitors the health and status of the satellites. It consists of six monitoring stations located in Cape Canaveral, Ascension Island, Kwajalein, Diego Garcia, Hawaii, and Colorado Springs. The four first also have each its ground antenna. These stations send clock corrections and orbital model to the satellites via the antennas.
- The user segment is the GPS reciever. In order to work, it needs an antenna tuned in to the frequencies used by the satellites. The reciever also has a high accuracy clock, usually being driven by a quarts oscillator.

The GPS transmits data signal over two main carrier frequencies, called L1 and L2, transmitting on 1575.42 and 1227.60 MHz respectively. All data is trasmitted using the Coarse/Acquisition (C/A) code, which is available to the public, and the Precise (P) code used by the military. L1 transmits both the C/A and the P code, while L2 transmits the P code. Both frequencies are available for all users, but due to encryption of the P code, only the C/A is usable by the public.

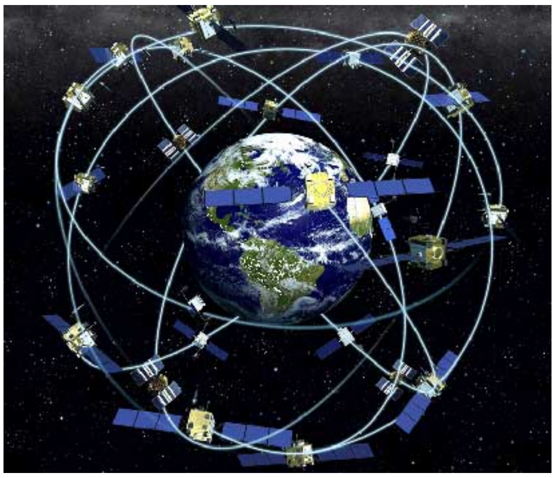

Figure 3.1: Concept art of the Global Positioning System [3].

3.2.1 Error Sources

As the GPS signals travel with the speed of light[5], an error of $\frac{1}{1000}$ms will lead to a measurement error of 300 m. Thus the timing needs to be highly accurate in order to give an acceptable measurement. The time bias can be assumed equal for all satellites and accounted for by using the measurement from three satellites simultaneously (solving four equations with four unknown variables). In other words, a minimum of four satellites are needed in order to achieve position.

However, several factors still contribute to the GPS error. It is appropriate to separate the error sources into two main groups; common mode and non-common mode errors [9]. Common mode errors are errors that occur within a limited geographic region and are equal for all recievers within the region. As opposed to common mode, non-common mode errors refer to reciever individual errors that can occur independent of location.

Receiver Clock Bias

Table 3.2 shows a list of errors, divided into common mode and non-common mode. One error that is not included in this list is the receiver clock bias. This error is equal for all signals, and can therefore be estimated if signals from four satellites are available by:

[5]Approximately $3 \cdot 10^8$m/s

Errors	Standard Deviation
Common Mode	
Selective Availability	24.0
Ionosphere	7.0
Clock and ephemeris	63.6
Troposphere	0.7
Noncommon Mode	
Reciever Noise	0.1-0.7
Multipath	0.1-3.0

Table 3.2: GPS Error Sources, reproduced from [9].

1. Differentiating two simoultaneous measurements from the same receiver
2. Calculating an estimate at each time step
3. Estimating the error as a state using a dynamic model and Kalman filtering

Although not in Table 3.2, this error is receiver individual, and can be viewed as non-common mode.

Atmospheric Effects

One problem with calculating the distance from the satellite based on the time a signal uses on its journey from the satellite to the receiver is that the signal has different speed based on the substance it travels through. This also applies for the Earth's atmosphere, and particularly the ionosphere. However, as the speed of signals in this layer is dependent on frequency[6], a two-frequency receiver can estimate this error easily. For a single-frequency receiver, the estimate is dependent on atmospheric modelling.

The different layers of the atmosphere can be viewed in Figure 3.2

The ionosphere is the upmost part of the atmosphere, and is ionized by solar radiation. From the display given in Figure 3.2, it is located within the Thermosphere.

As atmospheric errors are dependent on the distance the signal travels through the atmosphere, they are smallest when the satellite is positioned straight

[6]This phenomenon is also known as dispersion

above the receiver. The more correct the estimated position is, the more accurately the atmospheric error can be calculated.

Another atmospheric error is the tropospheric delay, which is dependent on atmospheric pressure, temperature, humidity and satellite elevation. This delay is usually separated into a wet and a dry component, where the dry component contributes to approximately 90 % of the delay. This component is relatively well modelled, while the wet one is more complicated due to many local factors. There are several different models for the tropospheric delay, which are good or bad depending on the angle of the satellite. As opposed to the ionospheric error, the tropospheric delay is not frequency dependent and more locally varying, making it difficult to estimate.

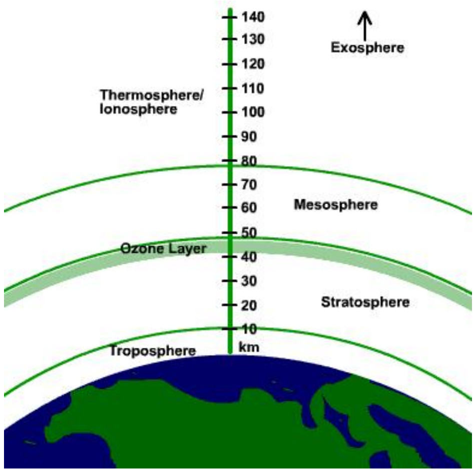

Figure 3.2: Illustration of Earth and its atmosphere [6].

Selective Availability

Selective Availability (SA) is an artificial feature designed by the U.S. Department of Defense. Its purpose is to introduce slowly changing random errors to avoid the GPS being used for military purposes (by other than the U.S.) or terrorist activites. However, this feature is currently disabled (since 2000), and will therefore not be discussed further.

Multipath

Multipath errors are a result of signals reflected off surfaces on the way to or in the vicinity of the receiver, causing the signal to travel further than the direct path, thus causing it to use a longer time to the receiver or the same signal to arrive twice. C/A multipath errors are usually from 0.1 - 3 m, but errors up to 100 m have been reported. For L1 carrier phase, the error is assumed to be less than 5 cm.

Should a signal arrive either twice after a newer signal due to multipath, the old signal will simply be neglected. However, if the signal simply is delayed and no other signals arrive at the receiver in the mean time, it is nearly impossible to separate the error from other errors. However, some precautions can be made:

- Using an antenna with low gain at low and negative elevations, due to most reflecting surfaces being below the receiver
- If possible, place the receiver higher than the highest reflector
- Do not accept signals from satellites at low elevation, as these travel nearly parallell to the surface and are thus more error-prone to reflections

Avoiding multipath is extremely important when choosing sites for DGPS reference stations, as multipath errors are non-common mode errors, and will manifest themselves in the error estimate sent from the station.

Receiver Noise

The receiver noise is assumed to be white, and is a result of error in measuring transit time. The error is due to factors such as nonlinearity and thermal noise. It is highly dependent on hardware selection in the receiver, and will therefore vary with the quality of the GPS receiver.

3.2.2 Differential GPS

As seen from Table 3.2, the most significant contribution to the error on the estimated position comes from the common-mode errors. By setting up a stationary reciever at a known position, the readings will be affected by the same common-mode errors as any other reciever in the area. Since the position is already known, the error can be calculated by subtracting the measurement from the receiver by the known position. This error can be broadcasted together with the corresponding clock readings. Thus, every receiver in the vicinity can obtain the error and adjust for it. The error calculated by the reference station will be assumed to be the common-mode error and is subtracted from the measurement.

The disadvantage of using DGPS is the lack of global coverage.

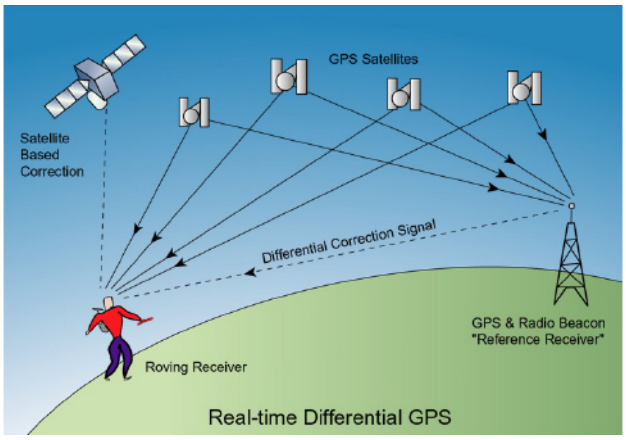
GPS Satellites
Satellite Based Correction
Differential Correction Signal
GPS & Radio Beacon "Reference Receiver"
Roving Receiver
Real-time Differential GPS

Figure 3.3: Graphical presentation of differential GPS [14].

The United Stated Federal Aviation Administration (FAA) and the United States Department of Transportation (DoT) has constucted a feature called the Wide Area Augmentation System (WAAS) [7]. Described shortly, WAAS is similar to the DGPS system, but only accessible in North-America and is mainly designed for aerial applications. WAAS is not certified for maritime navigation, and it is claimed that DGPS has a higher accuracy whenever close to the reference station. Due to WAAS being unavailable outside North-America, and the fact that it has not yet been certified for marine applications [7], it will not be discussed further.

3.2.3 Velocity Measurements

Navigational charts and other tools such as GPS measurements are usually given in an ECEF geodetic reference frame, using latitude, longitude and altitude, denoted as $[\Phi, \lambda, h]$ respectively. For presentation or using as aid to an INS, both ECEF and a local geodetic frame can be used. The local geodic frame is usually preferred whenever operating within a small area. For larger areas of operation, ECEF is concidered inertial.

There are several ways to perform the integration between GPS and INS, depending on the frame desired. In this report, integration is performed in two different frames, depending on the measurement. For position, ECEF geodetic (Φ, λ, h) is used, while for speed, the tangent-plane (NED) has been chosen.

In order to transform the GPS data, the position, already given in ECEF geodetic coordinates, is differentiated. To transform the speed, (3.31) is used,

$$\begin{bmatrix} \dot{\Phi} \\ \dot{\lambda} \\ \dot{h} \end{bmatrix} = \begin{bmatrix} \frac{1}{R_\Phi + h} & 0 & 0 \\ 0 & \frac{1}{(R_\lambda + h)cos(\Phi)} & 0 \\ 0 & 0 & -1 \end{bmatrix} \begin{bmatrix} v_N \\ v_E \\ v_D \end{bmatrix} \tag{3.40}$$

$$\begin{bmatrix} v_N \\ v_E \\ v_D \end{bmatrix} = \begin{bmatrix} R_\Phi + h & 0 & 0 \\ 0 & (R_\lambda + h)cos(\Phi) & 0 \\ 0 & 0 & -1 \end{bmatrix} \begin{bmatrix} \dot{\Phi} \\ \dot{\lambda} \\ \dot{h} \end{bmatrix}, \tag{3.41}$$

where R_Φ and R_λ is given in (3.32)–(3.33).

3.3 Hardware Selection

As this report will consider the implementation of an integrated navigation system, hardware is needed. The IMU has been chosen mainly according to price, while the GPS module has been recycled from an earlier Unmanned Aerial Vehicle (UAV) project at NTNU [8].

3.3.1 IMU

The IMU chosen is the Microstrain 3DM–GX1. This consists of three accelerometers, three gyros and three magnetometers, thus giving acceleration in 6 degrees of freedom (6 DOF) and position in 3 DOF.

Figure 3.4: Microstrain 3DM–GX1 IMU [12].

The 3DN–GX1 guarantees an accelerometer bias stability of 0.010 G, where G is the Earth's gravitational constant, and 0.7°/sec for the gyros. To correct the gyro error, the magnetometers can be used, operating at a bias stability of 0.010 gauss. The sensors have a bandwidth of 100 Hz, and are able to detect accelerations up to 500 G.

The IMU transmits data over an RS–232 serial line, depending on the command sent to the device. As a standard, the 3DN–GX1 transmits a message each time the given command byte is sent, but continuous mode can be enabled, making the IMU transmit a given message continuously.

3.3.2 GPS Receiver

The GPS module, as mentioned earlier, has been recycled from a UAV project detailed in [8]. The GPS consists of a GlobalSat EM–411 receiver mounted on a RS–232 interface, as shown in Figure 3.5.

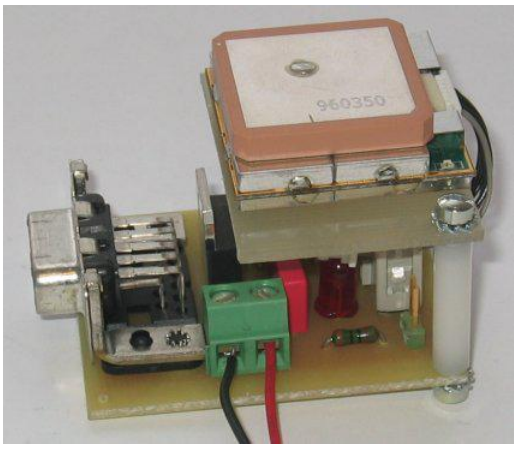

Figure 3.5: GlobalSat EM–411 GPS receiver with the RS–232 interface.

The module has no internal power, and thus needs external powering to function. It operates at 4.5 – 6.5 V, but the RS–232 board contains a voltage converter, making it able to operate at 9 V, meaning it can be powered by an external 9 V power supply or a PP3 battery, most commonly used in smoke detectors.

This receiver has a position accuracy of 10 meters, or 5 meters with Wide Area Augmentation System (WAAS) enabled. The EM–411 module does support DGPS, but its manual does not list the accuracy for DGPS. However, the accuracy can be assumed close to that of WAAS.

The EM-411 receiver supportes NMEA 0183 protocol, which is also the standard setting, discussed in Section 3.3.3.

The price of the EM–411 is less than 500 NOK. More data on the module is provided in Appendix A. For hardware-interested readers, the full EM–411 manual is available at [5].

3.3.3 NMEA 0183

The NMEA 0183 is a standard developed by the National Marine Electronics Association and uses ASCII communication over the serial line. The standard is commonly used in marine measurement devices like GPS receivers. The message header can be divided in three parts; first, a $-sign implying the start of a message followed by a prefix containing a device identifier specified by the protocol. The final three letters contain the type of message being sent, however only two are particularly relevant for obtaining the position, hence GGA and RMC. Only these two will be explained in the following text. More information can be found in [2].

The GGA suffix denotes the "Global Positioning System Fix Data". It contains time, position and fix related data for a GPS receiver. Table 3.3 shows a GGA message with a description of each message part. For messages using the NMEA 0183 standard, each part of the message are separated with the ',' delimiter.

The RMC suffix indicates the contents of the message being the "Recommended Minimum Navigation Information". An example message is shown in Table 3.5.

Name	Example	Description
Message ID	$GPGGA	Message header
Time (UTC)	123456.123	[hhmmss.sss]
Latitude	6325.0840	[ddmm.mmmm]
N/S Indicator	N	North (N) or South (S)
Longitude	01024.1304	[dddmm.mmmm]
E/W Indicator	E	East (E) or West (W)
GPS Quality Indicator	1	See Table 3.4
Number of satellites	09	00 - 12
HDOP	2.1	Horizontal dilution of precision
Altitude	56.1	Altitude relative to geoid
Units	M	Units of antenna altitude
Geoidal separation	10.1	WGS-84 height deviation
Units	M	Units of geoidal separation
Age of diff. GPS data		Null field without DGPS
Diff. ref. station ID	0000	0000-1023
Checksum	*6B	

Table 3.3: The NMEA GGA message [2].

Value	Description
0	Fix not available or invalid
1	GPS SPS Mode, fix valid
2	Differential GPS, SPS mode, fix valid
3	GPS PPS Mode, fix valid

Table 3.4: GPS Quality Indicator Values [2].

Name	Example	Description
Message ID	$GPRMC	Message header
Time (UTC)	123456.123	[hhmmss.sss]
Status	A	A = data valid, V = data invalid
Latitude	6325.0840	[ddmm.mmmm]
N/S Indicator	N	North (N) or South (S)
Longitude	01024.1304	[dddmm.mmmm]
E/W Indicator	E	East (E) or West (W)
SOG	0.16	Speed over ground [knots]
COG	46.98	North relative to north [deg]
Date	220508	[ddmmyy]
Magnetic variation	E	East or West [deg]
Checksum	*6B	

Table 3.5: The NMEA RMC message [2].

Chapter 4

Integrating GPS and INS

4.1 Approaches

There are several ways to implement a GPS/INS integration. First of all, we differ between the direct-filtering and the complementary-filtering approach [9].

4.1.1 Direct-Filtering

Direct-filtering is perhaps the most intuitive of the two. It uses position and velocity as states in a state space representation, with GPS data as measurements (y) and the inertial measurements as input (u) in a Kalman filter. While this seems straight forward, it has three major drawbacks:

1. The Kalman filter covariance equations have to be calulated at the rate of the inertial measurements. As these equations require much CPU, the bandwith of the inertial measurements are highly restricted
2. The measurements have highly deterministic components that will be represented by ad hoc models in the state space representation.
3. The states can change dramatically between iterations, which require high filter bandwith.

Complementary-filtering considers the inertial measurements and mechanization equations as two separate systems, giving the Kalman filter a reference trajectory. When new GPS measurements arrive, the INS states are compared to the GPS data. By running the difference between the two sets of data through a second Kalman filter, a set of error equations can be estimated.

This implementation enables the covariance update equations to be calculated only at each GPS measurement, reducing the total computational load.

4.1.2 Complementary-Filtering

For the complementary-filtering approach, there are three different solutions, loosely coupled GPS position and range aided INS, plus a tightly coupled approach.

The loosely coupled GPS position aided INS is shown in Figure 4.1. This method uses the position from the GPS to calculate the INS error, which is fed back to the INS system. This method is very simple and requires little processing of the GPS output.

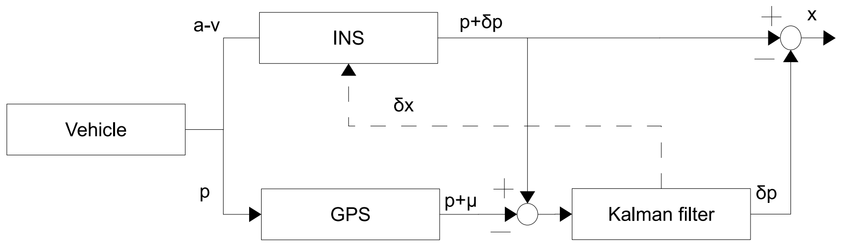

Figure 4.1: GPS position aided INS [9].

A similar method is the GPS range aided INS, shown in Figure 4.2. This method uses a range predictor to transform the INS measurements to a range prediction, while comparing these to the GPS range measurements. This approach gives a better system performance than the position aided system, but requires the understanding and processing of GPS data, which may be unavailable for off-the-shelf hardware.

Finally, the tightly coupled solution uses INS data as feedback also to the GPS. This decreases the bandwith of the tracking loop, and makes the system less prone to interference and jamming. However, this approach requires not only access to the range data, but also to the hardware and Kalman filter design in the GPS. Thus, this approach is generally not available when using an off-the-shelf receiver.

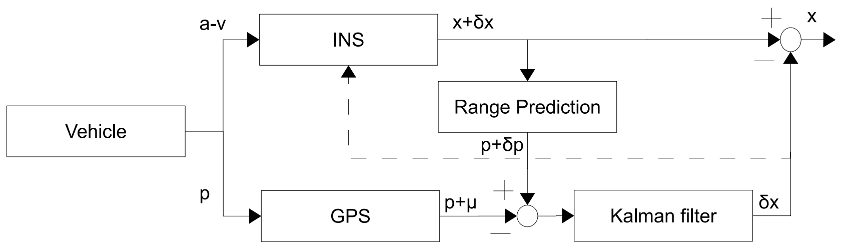

Figure 4.2: GPS range aided INS [9].

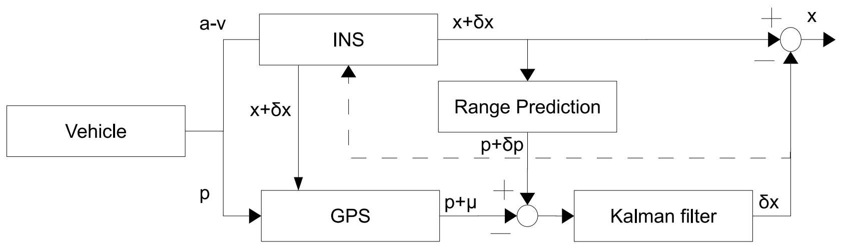

Figure 4.3: Tightly coupled GPS aided INS [9].

4.2 GPS Position Aided INS

The GPS position aided INS is defined as an INS using the GPS position to adjust for the drifting due to INS acceleration error [9]. It is useful to put the system equations on state space form

$$\dot{\mathbf{x}} = \mathbf{A}\mathbf{x} + \mathbf{B}\mathbf{u} + \mathbf{f}(\mathbf{x},\mathbf{u}) + \mathbf{D}\boldsymbol{\nu} \tag{4.1}$$

$$\mathbf{y} = \mathbf{C}\mathbf{x} + \mathbf{w}, \tag{4.2}$$

where $\mathbf{x}$ is the states, $\mathbf{u}$ is the input, **f(x,u)** is the non linear parts of the differential equation, $\boldsymbol{\nu}$ is the process noise and $\mathbf{w}$ is the measurement noise.

Combining (3.27) with (4.1), using $\mathbf{x} = \begin{bmatrix} \mathbf{p} & \mathbf{v} \end{bmatrix}^T$, the system can be written as

$$\dot{\mathbf{x}}^t = \begin{bmatrix} \mathbf{0} & \mathbf{I} \\ \mathbf{0} & \mathbf{0} \end{bmatrix} \mathbf{x}^t + \begin{bmatrix} \mathbf{0} \\ \mathbf{R}_p^t(\bar{\mathbf{f}}^p + \mathbf{b}^p) - \mathbf{g}^t \end{bmatrix} + \begin{bmatrix} 0 \\ (\boldsymbol{\Omega}_{et}^t - 2\boldsymbol{\Omega}_{ie}^t)\mathbf{v}^t \end{bmatrix} \tag{4.3}$$

where $\mathbf{b}^p$ is the accelerometer bias, calculated in the Kalman filter and

$$\boldsymbol{\omega}_{et}^t + 2\boldsymbol{\omega}_{ie}^t = \begin{bmatrix} (\dot{\Phi} + 2\omega_{ie})cos(\lambda) \\ -\dot{\lambda} \\ -(\dot{\Phi} + 2\omega_{ie})sin(\lambda) \end{bmatrix} \tag{4.4}$$

For simplicity, $\mathbf{I}$ and $\mathbf{0}$ is used throughout this document, meaning $\mathbf{I}_{3\times 3}$ and $\mathbf{0}_{3\times 3}$ unless stated otherwise[1]. The input, $\mathbf{u}$, is the measured force from the INS, $\bar{\mathbf{f}} = \mathbf{f} + \tilde{\mathbf{f}}$.

For a simpler transition between GPS and INS states, (4.3) can be rewritten to give its position in ECEF geodetic coordinates (Φ, λ, h). This is easilly achieved using $\mathbf{R}_t^{E_g}$ given in (3.31), yielding

$$\dot{\mathbf{x}}^n = \begin{bmatrix} \mathbf{0} & \mathbf{R}_t^{E_g} \\ \mathbf{0} & \mathbf{0} \end{bmatrix} \mathbf{x} + \begin{bmatrix} \mathbf{0} \\ \mathbf{R}_p^n(\bar{\mathbf{f}}^p - \mathbf{b}^p) - \mathbf{g}^n \end{bmatrix} + \begin{bmatrix} 0 \\ (\boldsymbol{\Omega}_{et}^t - 2\boldsymbol{\Omega}_{ie}^t)\mathbf{v}^t \end{bmatrix} \tag{4.5}$$

$$\mathbf{y} = \begin{bmatrix} \mathbf{I} & \mathbf{0} \end{bmatrix} \mathbf{x} + \mathbf{w}, \tag{4.6}$$

Combining these equations, the resulting equations yields

$$\dot{\mathbf{v}}^t = \bar{\mathbf{f}}^t - \mathbf{b}^t + \mathbf{g}^t + \begin{bmatrix} -(\dot{\Phi} + 2\omega_{ie})sin(\lambda)v_E + \dot{\lambda}v_D \\ (\dot{\Phi} + 2\omega_{ie})sin(\lambda)v_N + (\dot{\Phi} + 2\omega_{ie})cos(\lambda)v_D \\ -(\dot{\Phi} + 2\omega_{ie})cos(\lambda)v_E + \dot{\lambda}v_N \end{bmatrix} \tag{4.7}$$

$$\dot{\mathbf{p}}^{E_g} = \mathbf{R}_t^{E_g}\mathbf{v}^t = \begin{bmatrix} \frac{1}{R_\lambda + h} & 0 & 0 \\ 0 & \frac{1}{(R_\Phi + h)cos(\lambda)} & 0 \\ 0 & 0 & -1 \end{bmatrix} \mathbf{v}^t \tag{4.8}$$

[1]This applies only for the boldfaced notation.

The bias calculation will be discussed later in this chapter.

The relationship between the measured and true output from the INS can be written as

$$\bar{\mathbf{f}}^p = \mathbf{f}^p + \tilde{\mathbf{f}}^p \tag{4.9}$$

$$\bar{\boldsymbol{\omega}}^p_{np} = \boldsymbol{\omega}^p_{np} + \tilde{\boldsymbol{\omega}}^p_{np}, \tag{4.10}$$

where the the error equation is given as [9]

$$\tilde{\mathbf{f}}^p = \tilde{\mathbf{A}}_a \mathbf{f}^p + \delta\mathbf{b}_a + \delta\mathbf{nl}_a + \boldsymbol{\nu}_a \tag{4.11}$$

$$\tilde{\boldsymbol{\omega}}^p_{ip} = \delta\mathbf{A}_g \boldsymbol{\omega}^g_{ip} + \delta\mathbf{b}_g + \delta\mathbf{nl}_g + \boldsymbol{\nu}_g. \tag{4.12}$$

These equations are also known as the truth model, where

- $\delta\mathbf{b}$ is a random walk variable, e.g. $\delta\dot{\mathbf{b}} = \boldsymbol{\nu}_b$ where $P_b(\boldsymbol{\nu}) = 0$
- $\delta\mathbf{nl}$ represents all the non linear errors
- $\boldsymbol{\nu}$ is the measurement noise
- $\delta\mathbf{A}$ is due to misalignment of the IMU

The misalignment matrix is given as

$$\delta\mathbf{A}_a = \begin{bmatrix} \delta SF_u & -\delta a_{uw} & \delta a_{uv} \\ \delta a_{vw} & \delta SF_v & -\delta a_{vu} \\ -\delta a_{wv} & \delta a_{wu} & \delta SF_w \end{bmatrix}$$

$$\delta\mathbf{A}_g = \begin{bmatrix} \delta SF_p & -\delta a_{pr} & \delta a_{pq} \\ \delta a_{qr} & \delta SF_q & -\delta a_{qp} \\ -\delta a_{rq} & \delta a_{rp} & \delta SF_r \end{bmatrix},$$

and $\delta\mathbf{nl}$ is the nonlinear error, given as

$$\delta\mathbf{nl}_a = \begin{bmatrix} k_{x1}f_u^2 + k_{x2}f_v^2 + k_{x3}f_w^2 + k_{x4}f_uf_v + k_{x5}f_vf_w + k_{x6}f_wf_x \\ k_{y1}f_u^2 + k_{y2}f_v^2 + k_{y3}f_w^2 + k_{y4}f_uf_v + k_{y5}f_vf_w + k_{y6}f_wf_x \\ k_{z1}f_u^2 + k_{z2}f_v^2 + k_{z3}f_w^2 + k_{z4}f_uf_v + k_{z5}f_vf_w + k_{z6}f_wf_x \end{bmatrix}$$

$$\delta\mathbf{nl}_g = \begin{bmatrix} k_{p1}f_p^2 + k_{p2}f_q^2 + k_{p3}f_r^2 + k_{p4}f_uf_v + k_{p5}f_vf_w + k_{p6}f_wf_u \\ k_{q1}f_p^2 + k_{q2}f_q^2 + k_{q3}f_r^2 + k_{q4}f_uf_v + k_{q5}f_vf_w + k_{q6}f_wf_u \\ k_{r1}f_p^2 + k_{r2}f_q^2 + k_{r3}f_r^2 + k_{r4}f_uf_v + k_{r5}f_vf_w + k_{r6}f_wf_u \end{bmatrix}.$$

Since the truth model gives a lot of parameters to be estimated, both the alingment error matrix **A**, and the nonlinear errors tend to be neglected to ensure proper observability. Furthermore, acceptable results are achieved using an error model of only slowly varying bias and white noise.

The bias differential equation should be modelled as

$$\dot{\mathbf{p}} = \boldsymbol{\nu}, \tag{4.13}$$

where $\boldsymbol{\nu}$ is white noise.

It is also worth noting that since the IMU chosen in this experiment includes a magnetometer, leading to the unit internally calculating position and angular velocity. Thus, the above equations regarding angular motion has not been used, as the IMU angular output was used directly.

4.2.1 GPS

Since the IMU position is already given in the ECEF geodetic frame, no transformation is required. However, the velocity vector needs to be transformed into the tangent-plane. This is an easy process, starting with differentiating two position measurements, obtaining the ECEF geodetic speed. By multiplying this with the matrix gained in (3.31), tangent-plane speed is achieved, For the GPS, its equations are already given in (3.41),

$$\begin{bmatrix} v_N \\ v_E \\ v_D \end{bmatrix} = \begin{bmatrix} R_\Phi + h & 0 & 0 \\ 0 & (R_\lambda + h)cos(\Phi) & 0 \\ 0 & 0 & -1 \end{bmatrix} \begin{bmatrix} \dot{\Phi} \\ \dot{\lambda} \\ \dot{h} \end{bmatrix}. \tag{4.14}$$

Thus the esimation error can be calculated as

$$\tilde{\mathbf{x}} = \mathbf{x}_{GPS} - \mathbf{x}_{IMU} \tag{4.15}$$

4.3 Kalman Filter

The Kalman filter is an optimal, linear state estimator, able to estimate the full system state, depending on incomplete and noisy measurement series. The theory of the filter dates back to 1960, when Rudolf Kalman proposed the filter to NASA for the Apollo Program. The filter comes in many different forms, but the one most relevant for this work is the discrete Kalman Filter, which also will be the one most thoroughly investigated.

4.3.1 Discrete Kalman Filter

The dicrete filter takes its basis in a system written on state-space form,

$$\mathbf{x}_{k+1} = \mathbf{A}_k\mathbf{x}_k + \mathbf{B}_k\mathbf{u}_k + \mathbf{D}_k\boldsymbol{\omega}_k \tag{4.16}$$

$$\mathbf{y}_k = \mathbf{C}_k\mathbf{x}_k + \boldsymbol{\nu}_k \tag{4.17}$$

with

$$\mathbf{Q}_k = E[\boldsymbol{\omega}_k\boldsymbol{\omega}_k^T] \tag{4.18}$$

$$\mathbf{R}_k = E[\boldsymbol{\nu}_k\boldsymbol{\nu}_k^T] \tag{4.19}$$

as covariant matrices for the process and measurement noise, respectively. It is assumed that both **Q** and **R** are known. As there are no input, **u**, in the system, this can be neglected.

Should the system be observable, the Kalman filter can be used. To ensure observability, the observability matrix,

$$\mathbf{O} = \begin{bmatrix} \mathbf{C} \\ \mathbf{C}_k\mathbf{A}_k \\ \cdot \\ \cdot \\ \cdot \\ \mathbf{A}_k^{n-1}\mathbf{C}_k \end{bmatrix}, \tag{4.20}$$

needs to have rank n, n being the number of states.

Should observability be obtained, the fiter process can begin, starting with estimation of the state variables,

$$\mathbf{x}_k^- = \mathbf{A}_{k-1}\mathbf{x}_{k-1}, \tag{4.21}$$

where $\mathbf{x}_{k-1}$ is the previously calculated state estimate. As the bias calculated in the filter is subtracted from the INS states, this previously calculated estimate needs to be reset every interation.

The process is repeated for the covariance matrix,

$$\mathbf{P}_k^- = \mathbf{A}_{k-1}\mathbf{P}_{k-1}\mathbf{A}_{k-1}^T + \mathbf{Q}_{k-1}. \tag{4.22}$$

With the estimated values in place, the Kalman gain and the covariance update can be calculated,

$$\mathbf{K}_k = \mathbf{P}_k^-\mathbf{C}_k^T[\mathbf{C}_k\mathbf{P}_k^-\mathbf{C}_k^T + \mathbf{R}_k]^{-1} \tag{4.23}$$

$$\mathbf{P}_k = \mathbf{I} - \mathbf{K_k}\mathbf{C_k}\mathbf{P_k^-}, \tag{4.24}$$

using the previously calculated estimates.

The Kalman gain are used to calculate the final estimate of the states

$$\mathbf{x}_k = \mathbf{K}_k[\mathbf{y}_k - \mathbf{C}_k\mathbf{x}_k^-] \tag{4.25}$$

Proper derivation of the filter equations can be found in [9], [10] or several other sources.

4.3.2 Integration Kalman Equations

The Kalman filter input, $\mathbf{y}$, is already given in (4.15). This can be used together with the knowledge of the error of the GPS and the INS data to derive the state space error equations.

As the Globalsat EM–411 fails to deliver sudo ranges, the GPS error is assumed only to be white noise, although not correct. For the IMU, it is already stated that the bias should be estimated as integrated white noise in addition to a white noise component directly on the signal to correspond to the measurement noise.

Using these assumptions together with the INS equations derived in 4.5, the model takes form as

$$\dot{\tilde{\mathbf{p}}}^{E_g} = \mathbf{R}_t^{E_g}\mathbf{v}^t \tag{4.26}$$

$$\dot{\tilde{\mathbf{v}}}^t = -\mathbf{b}^t + \boldsymbol{\nu}_a^t, \tag{4.27}$$

which can be rewritten as

$$\dot{\mathbf{x}} = \begin{bmatrix} \mathbf{0} & \mathbf{R}_t^{E_g} & \mathbf{0} \\ \mathbf{0} & \mathbf{0} & -\mathbf{I} \\ \mathbf{0} & \mathbf{0} & \mathbf{0} \end{bmatrix} \mathbf{x} + \begin{bmatrix} \mathbf{0} & \mathbf{0} \\ \mathbf{I} & \mathbf{0} \\ \mathbf{0} & \mathbf{I} \end{bmatrix} \boldsymbol{\nu} \tag{4.28}$$

$$\mathbf{y} = \begin{bmatrix} \mathbf{I} & \mathbf{0} & \mathbf{0} \\ \mathbf{0} & \mathbf{I} & \mathbf{0} \end{bmatrix} \mathbf{x} + \begin{bmatrix} \mathbf{I} & \mathbf{0} \\ \mathbf{0} & \mathbf{I} \end{bmatrix} \mathbf{w}, \tag{4.29}$$

where $\mathbf{x} = \begin{bmatrix} \tilde{\mathbf{p}}^{E_g} & \tilde{\mathbf{v}}^t & \mathbf{b}^t \end{bmatrix}^T$.

The estimated position and speed error are then subtracted from the original states calculated from the IMU measurements. As the bias is likely to be following each of the accelerometers, it needs to be transformed back to the platform frame immediatetly after calculated. This transformation is to be performed using the mean value of the attitude measurements, dating back to the previous filter update.

4.4 Equations Summary

To give a quick summary of the equations given earlier in the report to be used in the actual integration process. This section is reccomended to be read after having obtained an understanding of what has been written in the previous sections of this report, and is meant to be used as a reference for implementation. Furthermore, it will only assess the equations used in the actual implementation of the total system.

4.4.1 IMU

$$\dot{\mathbf{v}}^t = \mathbf{R}_p^t(\bar{\mathbf{f}}^p + b^p) + \mathbf{g}^t + \begin{bmatrix} -(\dot{\Phi} + 2\omega_{ie})sin(\lambda)v_E + \dot{\lambda}v_D \\ (\dot{\Phi} + 2\omega_{ie})sin(\lambda)v_N + (\dot{\Phi} + 2\omega_{ie})cos(\lambda)v_D \\ -(\dot{\Phi} + 2\omega_{ie})cos(\lambda)v_E + \dot{\lambda}v_N \end{bmatrix} \tag{4.30}$$

$$\dot{\mathbf{p}}^{E_g} = \mathbf{R}_t^{E_g}\mathbf{v}^t = \begin{bmatrix} \frac{1}{R_\lambda + h} & 0 & 0 \\ 0 & \frac{1}{(R_\Phi + h)cos(\lambda)} & 0 \\ 0 & 0 & -1 \end{bmatrix} \mathbf{v}^t \tag{4.31}$$

which is to be computed at each iteration.

4.4.2 GPS

For the GPS measurements, the speed needs to be derived and transformed to the tangent plane,

$$\mathbf{v}^t = \mathbf{R}_{E_g}^t\mathbf{v}^{E_g} = \begin{bmatrix} R_\lambda + h & 0 & 0 \\ 0 & (R_\Phi + h)cos(\lambda) & 0 \\ 0 & 0 & -1 \end{bmatrix} \mathbf{v}^{E_g}. \tag{4.32}$$

4.4.3 Kalman Filtering

Kalman filtering is applied whenever a GPS measurement arrives. The filtering is done with regard to the error equations,

$$\dot{\tilde{\mathbf{p}}}^{E_g} = \mathbf{R}_t^{E_g}\mathbf{v}^t \tag{4.33}$$

$$\dot{\tilde{\mathbf{v}}}^t = -\mathbf{b}^t + \boldsymbol{\nu}_a^n, \tag{4.34}$$

which can be written on state space form

$$\dot{\mathbf{x}} = \begin{bmatrix} \mathbf{0} & \mathbf{R}_t^{E_g} & \mathbf{0} \\ \mathbf{0} & \mathbf{0} & -\mathbf{I} \\ \mathbf{0} & \mathbf{0} & \mathbf{0} \end{bmatrix} \mathbf{x} + \begin{bmatrix} \mathbf{0} & \mathbf{0} \\ \mathbf{I} & \mathbf{0} \\ \mathbf{0} & \mathbf{I} \end{bmatrix} \boldsymbol{\nu} \tag{4.35}$$

$$\mathbf{y} = \begin{bmatrix} \mathbf{I} & \mathbf{0} & \mathbf{0} \\ \mathbf{0} & \mathbf{I} & \mathbf{0} \end{bmatrix} \mathbf{x} + \begin{bmatrix} \mathbf{I} & \mathbf{0} \\ \mathbf{0} & \mathbf{I} \end{bmatrix} \mathbf{w} \tag{4.36}$$

using $\mathbf{x} = \begin{bmatrix} \tilde{\mathbf{p}}^{E_g} & \tilde{\mathbf{v}}^t & \mathbf{b}^t \end{bmatrix}^T$.

These equations are put on discrete form and fed into the Kalman filter equations, given in (4.20)–(4.25),

$$\mathbf{x}_k^- = \mathbf{A}_{k-1}\mathbf{x}_{k-1} \tag{4.37}$$

$$\mathbf{P}_k^- = \mathbf{A}_{k-1}\mathbf{P}_{k-1}\mathbf{A}_{k-1}^T + \mathbf{Q}_{k-1} \tag{4.38}$$

$$\mathbf{K}_k = \mathbf{P}_k^-\mathbf{C}_k^T[\mathbf{C}_k\mathbf{P}_k^-\mathbf{C}_k^T + \mathbf{R}_k]^{-1} \tag{4.39}$$

$$\mathbf{P}_k = \mathbf{I} - \mathbf{K_k}\mathbf{C_k}\mathbf{P_k^-} \tag{4.40}$$

$$\mathbf{x}_k = \mathbf{K}_k[\mathbf{y}_k - \mathbf{C}_k\mathbf{x}_k^-]. \tag{4.41}$$

Furthermore, as the bias is subtracted from the respective states, the estimated bias needs to be set zero every iteration.

Chapter 5

Results

All simulations and tests have been performed in Matlab, using Runge-Kutta 4 for solving the differential equations. A c++ implementation has also been made for real time implementation, based on the existing code at Maritime Robotics, but this code had performance issues due to only using an old laptop with insufficient computation capabilities.

Also, due to this thesis being somewhat delayed, all results have been obtained during the summer vacation, meaning that any tests on a boat was hard to perform. Thus, all tests have been made within a small area, while attempting to simulate a USV-like environment.

At the Microstrain IMU, the z-axis is pointing upwards (despite the drawing on the IMU, telling it points down), meaning that the z-axis needs to be inverted. The other axis are correct as they are marked on the IMU, completing the right hand rule. Also the yaw angle seems to be measured against west instead of north, meaning $90°$ has to be subtracted from the yaw angle. Both the z-axis correction and the yaw angle correction are contrary to what stands in the manual, and it is unknown whether this is a manufacturing error.

Covarianse matrices has been found by sampling GPS and IMU measurements, and calculating the covariance offline.

All test results shown are taken from several samples in an attempt to capture the worst-case results. This is due to some of the tests results being result of pure luck, leading to a better performance then what can really be expected.

5.1 Stationary Tests

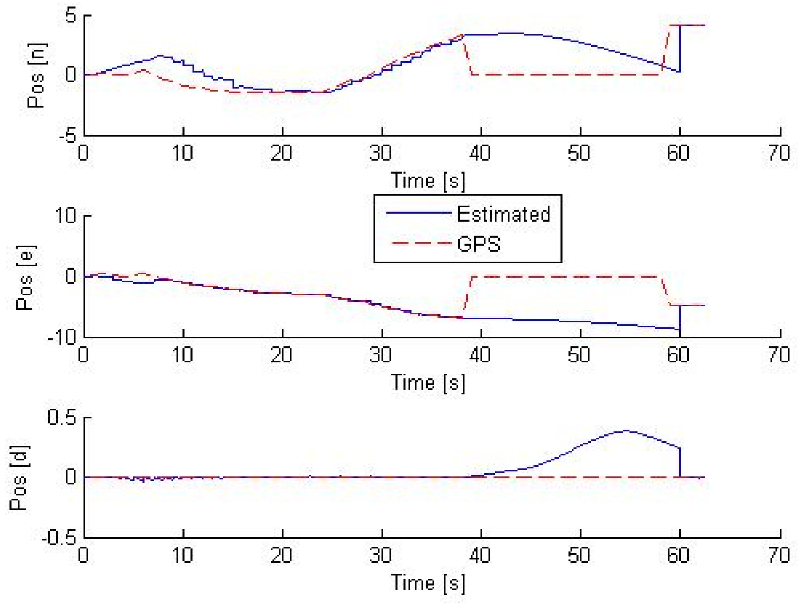

Figure 5.1: Stationary position wih GPS dropout.

For preliminary tests, both the IMU and the GPS receiver were kept stationary and the measurements were logged in Matlab. By using these measurements as input into the model found in the previous chapter, the equations were tested to determine any errors. At 40 to 60 seconds, the GPS disconnects.

This process were not done in real-time, solving another problem, hence the lack of proper computational hardware.

As can be seen from Figure 5.3 the acceleration estimates manage to converge towards 0, resulting in a maximum deviation of less than 10 meters after 40 seconds without GPS-aid in the east direction, the result shown in Figure 5.1.

Although these figures shows promising results, they should not be taken into to high regard however, as the system is stationary. However, they do show that the simplifications of the IMU equations is close to that of the truth model, and that the system performs satisfactory so far, as long as the GPS measurements are credible.

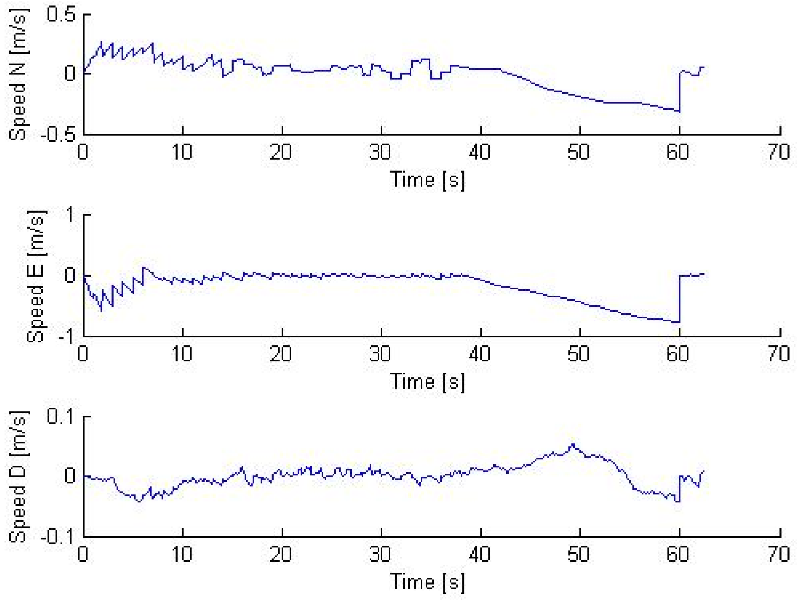

Figure 5.2: Stationary speed deviation with GPS dropout.

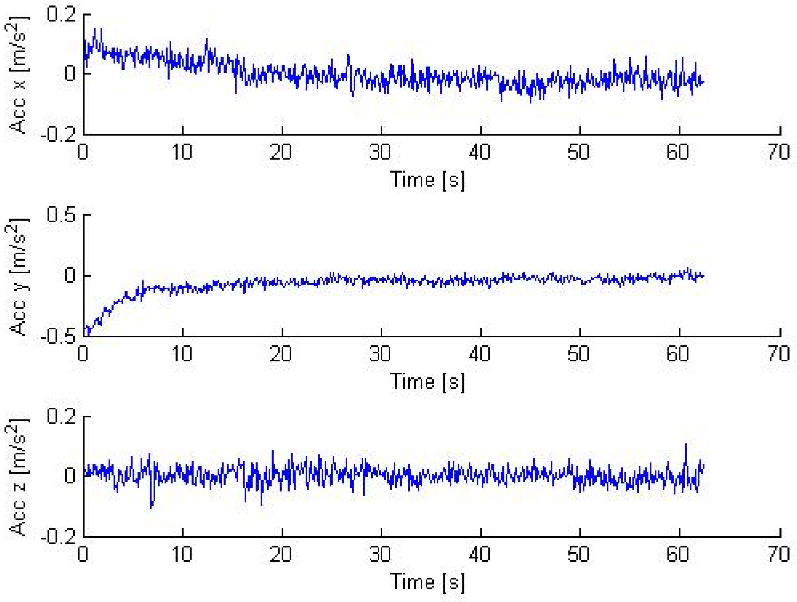

Figure 5.3: Stationary acceleration deviation with GPS dropout.

Table 5.1 shows the root mean square values of the deviation in acceleration, speed and position with the GPS being online.

	North/East	Down
Acceleration (RMS)	0.05	0.02
Velocity (RMS)	0.09	0.01
Position (RMS)	3	0.005

Table 5.1: RMS values, integrated INS/GPS in static conditions.

Calculating RMS values during GPS dropout would be pointless, as this will increase exponentially over time.

Comparing Table 5.1 with Figure 1.1, it is clear to see that the low cost application range within the specifications of the Crossbow NAV420, and is about twice to that of the Kongsberg Seatex Seapath 100 while being stationary, meaning that the success of the low cost application is feasible. It is worth noting however, that the down-component has such low Root Mean Square readings due to the altitude of the USV being assumed 0 whenever GPS measurements arrive.

5.2 Dynamic Tests

Next, it's time to test the system in motion. As no proper system were availiable for benchmarking, a previously known path were set up in order to test the performance.

After approximately 40 seconds, the IMU is assumed to be proper calibrated, and is moved in a square-like path of about 5×5 meters, always moving in the direction of IMU's x-axes. During the first run, the GPS is constantly online. The results is shown in Figures 5.4 – 5.6.

As can be seen from Figure 5.4, the position deviation is not that large. The measurements from the GPS are a bit to low according to the real path, whereas the true position lies somewhere in between the two. Regardless, the Kalman filter corrects the INS estimates quite conciderably, which can easily be seen from the speed estimates in Figure 5.5.

The estimated bias is shown in Figure 5.7

It may also be worth taking a look at Figure 5.8, showing the yaw angle measurement, which is quite accurate.

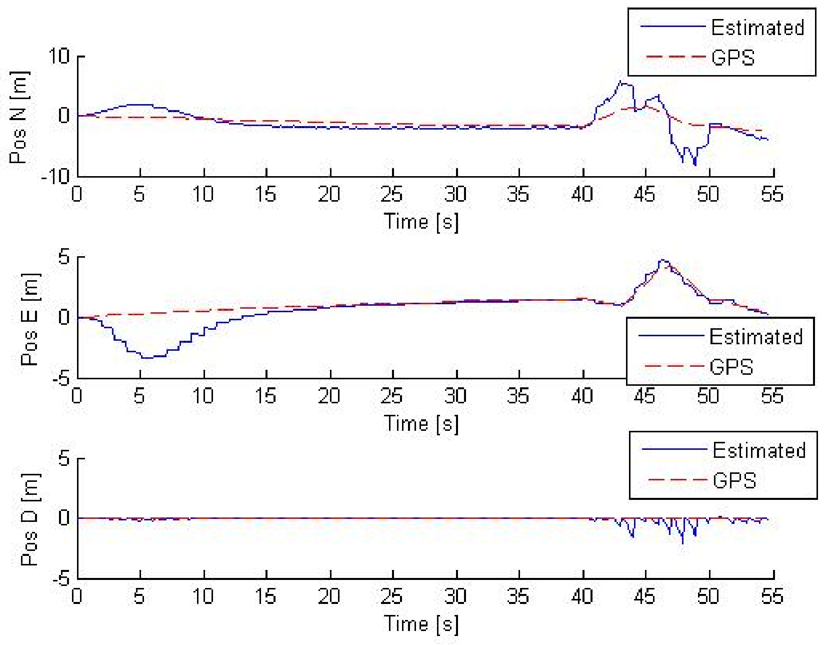

Figure 5.4: Dynamic postion estimate with GPS coverage.

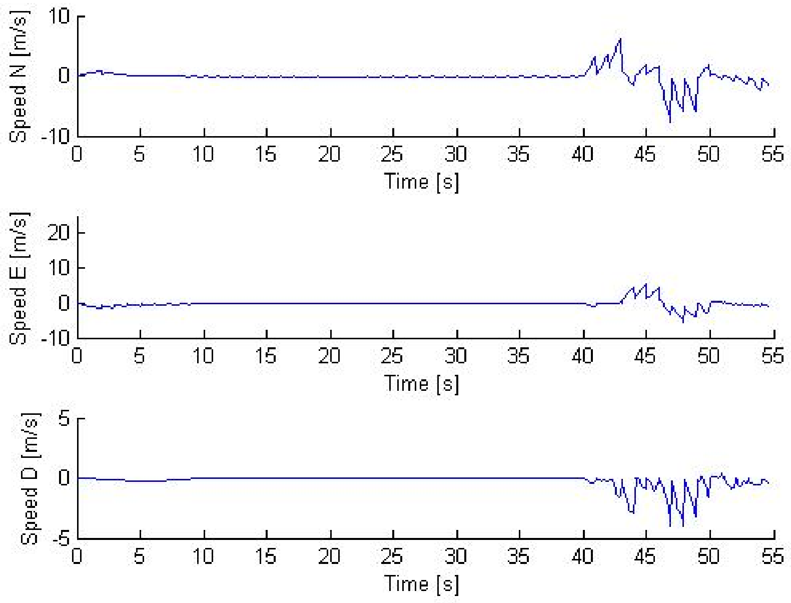

Figure 5.5: Dynamic speed estimate with GPS coverage.

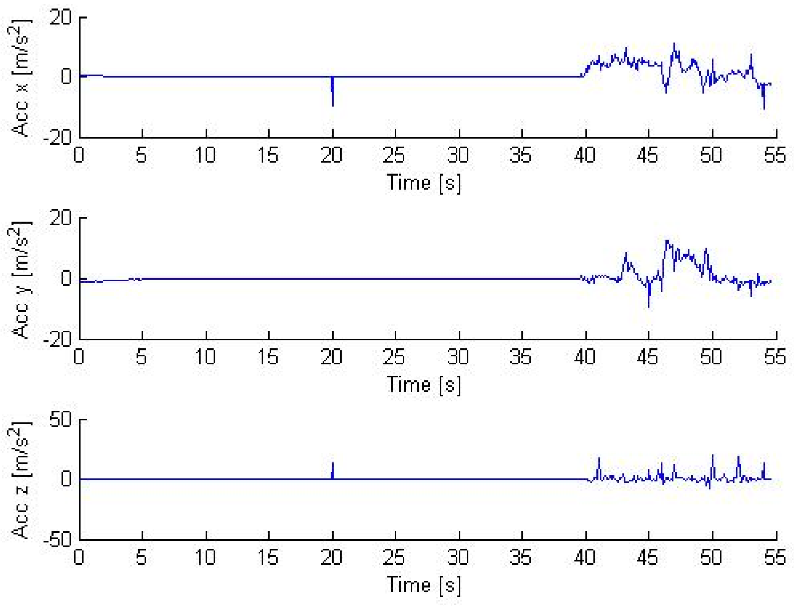

Figure 5.6: Dynamic acceleration estimate with GPS coverage.

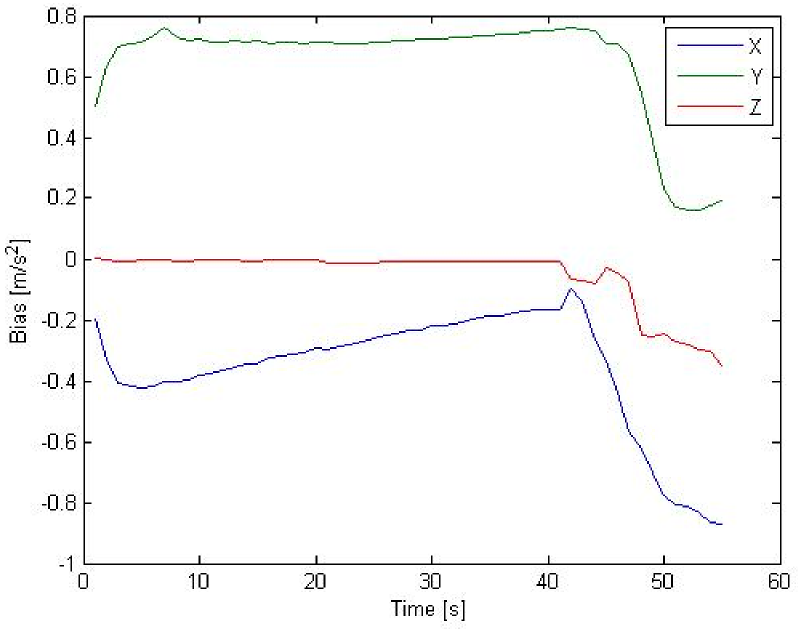

Figure 5.7: Bias estimate during dynamic conditions.

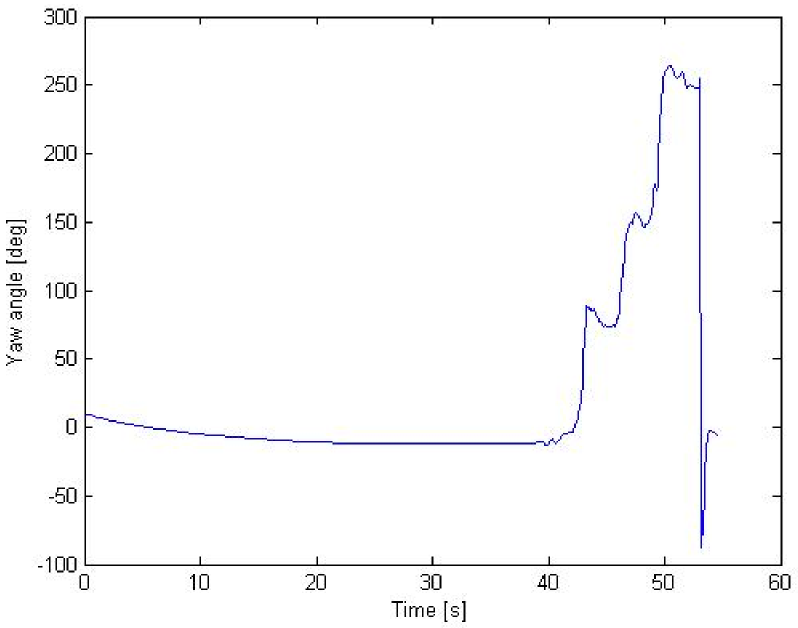

Figure 5.8: Measured yaw angle during dynamic conditions.

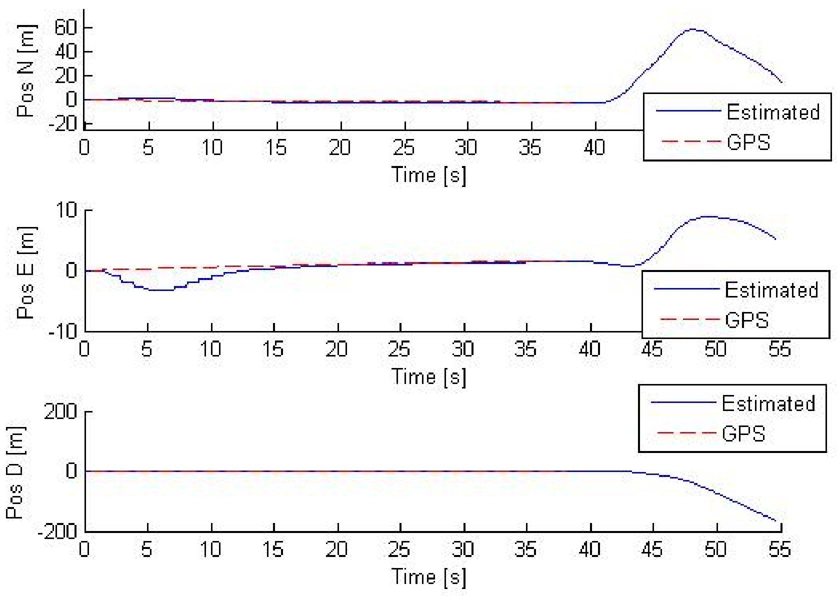

Figure 5.9: Dynamic postion estimate with GPS dropout.

Due to uncertainties on true position, it is hard to calculate the RMS correctly. By wrongfully using the GPS measurements as the correct position, the RMS values for the deviation can be calculated. The results are shown in Table 5.2. As can be seen, the position RMS is actually lower in north/east direction than it was during static conditions. This is merely due to the subtraction of the GPS position.

	North	East	Down
Velocity (RMS)	2.0428	1.4548	0.6307
Position (RMS)	2.1724	1.3248	0.3350

Table 5.2: RMS values, integrated INS/GPS while in motion

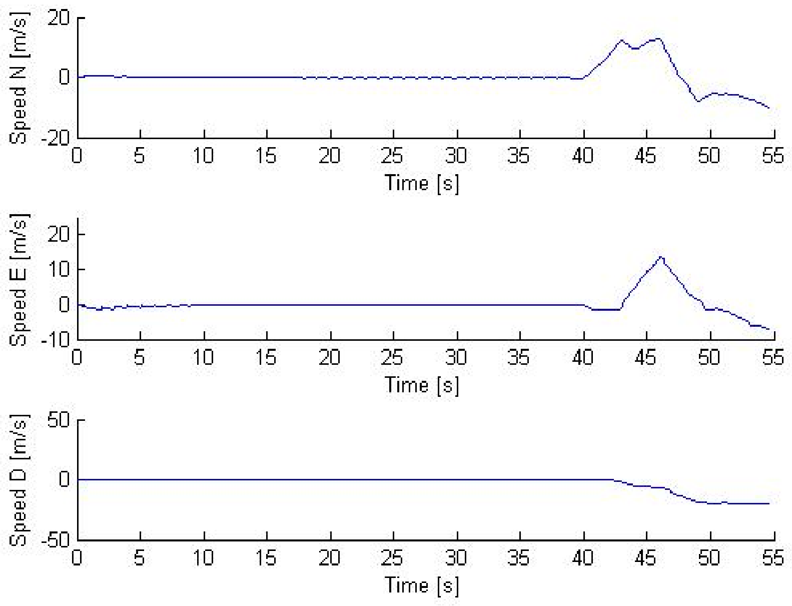

Figure 5.10: Dynamic speed estimate with GPS dropout.

It is also worth noting what happens when the GPS is offline during when moving through the course. As can be seen from Figures 5.9 and 5.10, the results are somewhat positive despite a high magnitude on the position, and a high drift downwards. Regardless, the deviation north and down are very large compared to what is really acceptable.

As the IMU is also supposed to be placed on a USV, it will also become subject to waves and vibrations. To simulate this, the IMU was kept nearly stationary, while being rotated and moved back and forth in small circles.

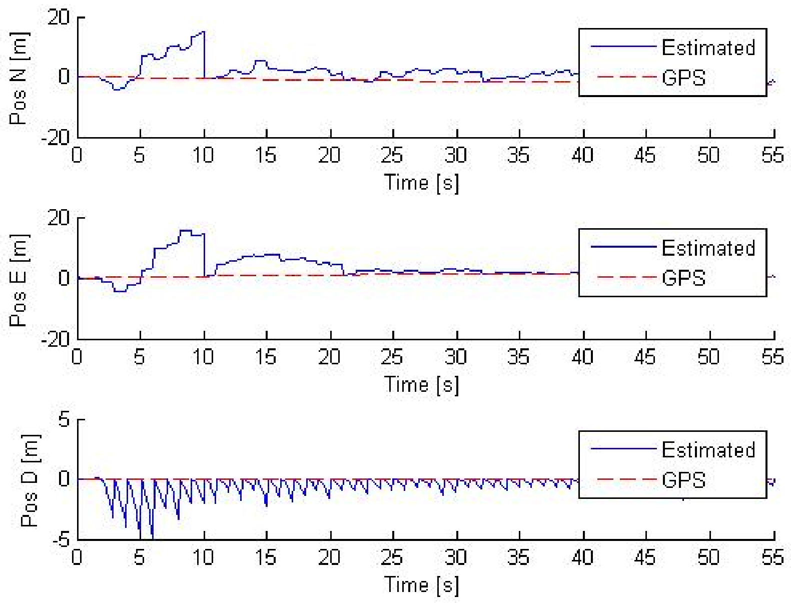

Figure 5.11: Position deviation during external influence, with GPS.

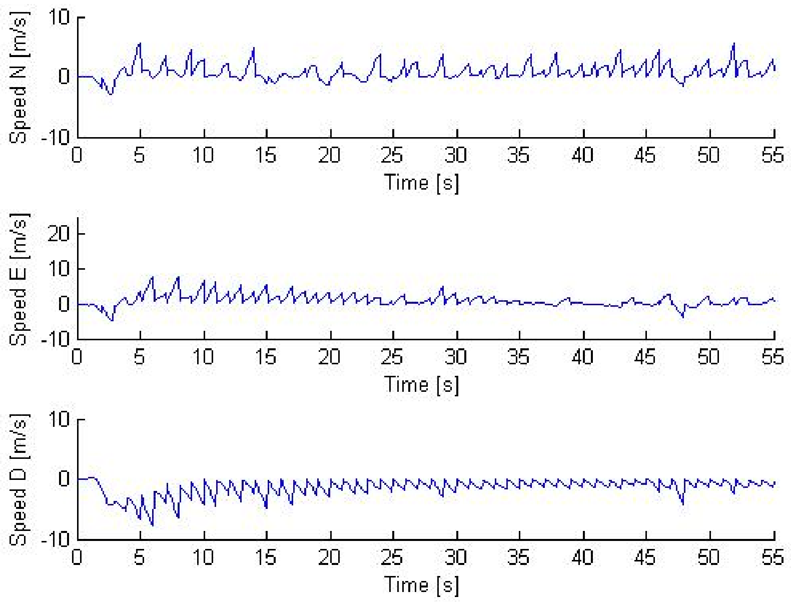

Figure 5.12: Speed deviation during external influence, with GPS.

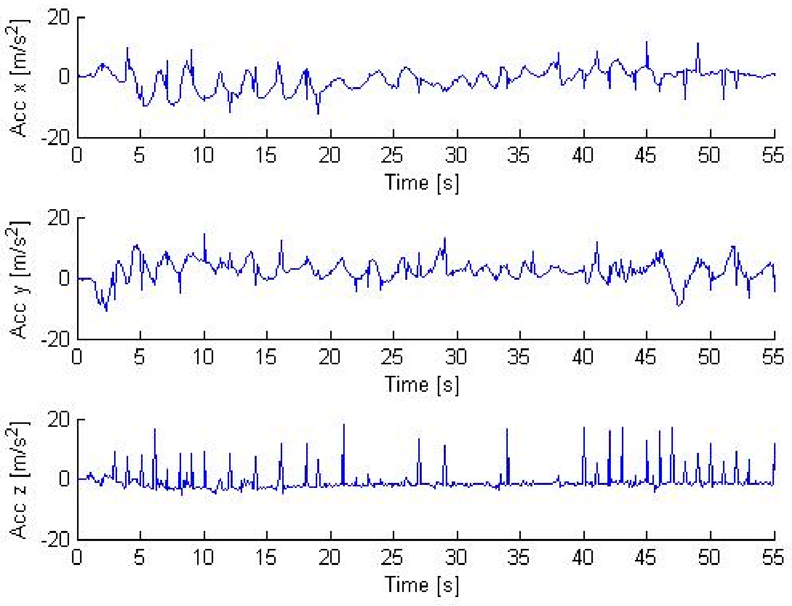

Figure 5.13: Acceleration during external influence, with GPS.

As seen from Figure 5.11 and 5.12, the estimate is able to follow the GPS relatively good, but struggles more than in the previous experiments. However, when GPS dropout is introduced, as seen in Figure 5.14 and 5.15, the estimate drifts off fast.

The RMS values for position and speed can be seen in Table 5.3.

	North	East	Down
Velocity (RMS)	1.3686	1.5217	1.3715
Position (RMS)	2.8322	2.8322	0.5399

Table 5.3: RMS values, integrated INS/GPS with external disturbances

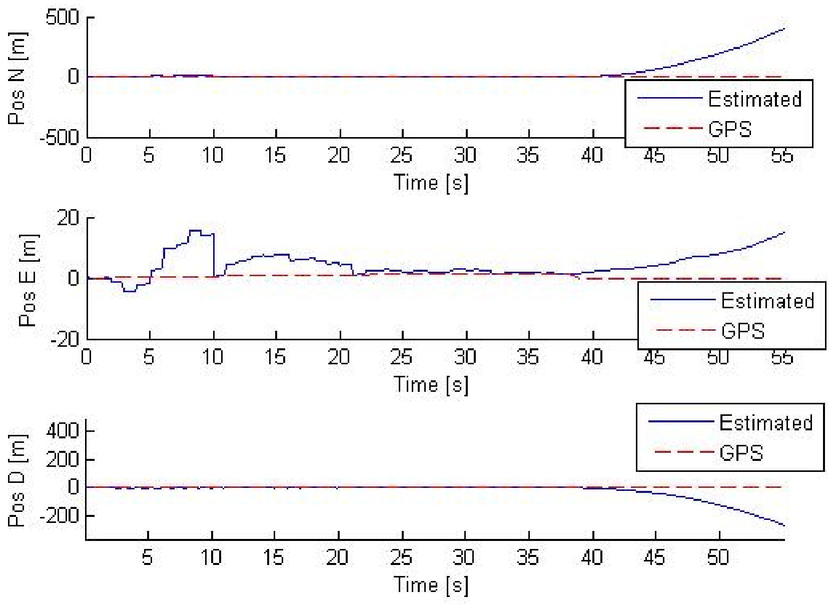

Figure 5.14: Position deviation during external influence, with GPS dropout.

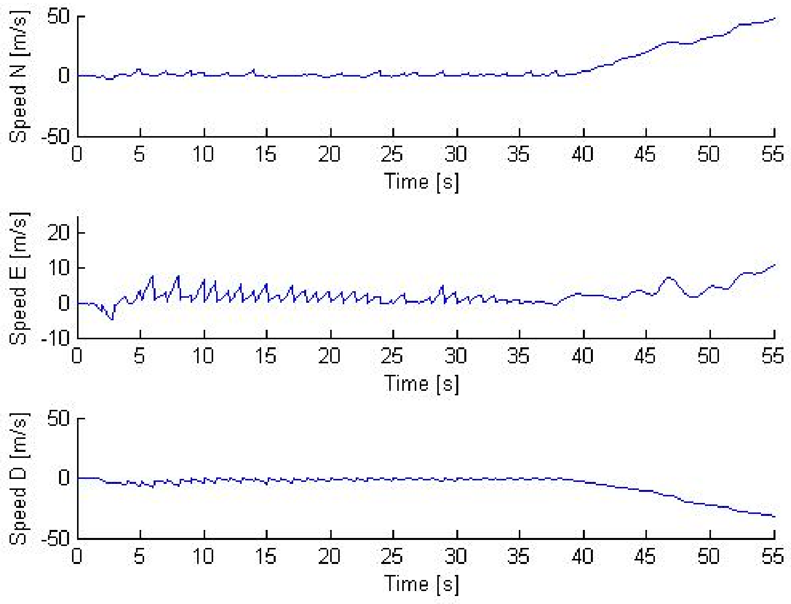

Figure 5.15: Velocity deviation during external influence, with GPS dropout.

Chapter 6

Discussion and Summary

6.1 Discussion

The low-cost application proved to work more or less satisfactory whenever GPS coverage were availiable. In static conditions it were also able to sustain long periods without GPS-aid, but whenever in motion of basically any kind, it starts to drift fast, even capable of obtaining several hundred meters deviation in just 20 seconds. With this kind of performance, it would be pointless to rely on the IMU delivering decent position estimates during GPS dropout. It could deliver satisfactory results when the vessel is subject only to small accelerations, but on a USV this is hardly ever the case.

However, when reviewing the deviation statistics and data plots from the previous chapter with the specifications of the Crossbow NAV420CA–100, a comparison can be made. As no drift characteristics are given, it is hard to draw any conclusions. The crossbow has a circular error of propability of 3, which actually is higher than using differential GPS, which usually operates at around 5 RMS[1]. The Crossbow velocity accuracy however, is about a third of the average RMS obtained in dynamic conditions, implying the IMU is of a higher standard which can also be seen directly from the acceleration accuracy on the IMU datasheet listed in Appendix A.

So, if any conclusion is to be made, the IMU is clearly not performing at such a level that any successful integration can be made, at least not for a USV. The application works satisfactory whenever GPS coverage is availiable, but during dropouts the IMU starts to drift fast and uncontrolled. The solution

[1]when assuming normal distribution, a CEP of 3 equals approximately 5 RMS.

could work to some extent in a car or similar, where the external noise on the vehicle is reduced, and there exists a set of feasable positions based on road networks, in addition to continously obtaining speed measurements from the vehicle.

The angular measurements are pretty accurate, and can be used directly as a compass. However, there has not been performed any corrections for position in the vincinity of the north pole to correct for the displacement of the magnetic north pole.

6.2 Future Work

First of all, if any further work is to be performed, it would be absolutely neccesary to invest in a more expensive IMU, since this lacks the performance to yield good results. Regardless of hardware, there are a few things that has not been implemented due to insufficeint time on the schedule:

- Quaternions should be used in stead of rotation matrices. This will lead to a lower computational load, as well as avoiding the singularity present at 90° pitch, even though this is as good as impossible on a USV.
- Temperature tests should be performed to determine the ratio between temperature and bias. IMUs are known to be more temperature dependant than time dependant, meaning the change in bias will be larger whenever there is a change in temperature than it will just over time.
- Obtaining a GPS receiver able to deliver pseudoranges, leading to the possibility of designing a tightly coupled integrated solution
- Using another, state of the art system, in order to benchmark the system properly

Appendix A

Data Sheets

The data sheets listed in this Appendix is taken from the specifications listed at the manufacturers' websites, and reproduced here in this report.

A.1 Microstrain 3DM–GX1

Orientation Range:	360° full scale (FS), all axes (Matrix, Quaternion modes)
Sensor Range	
Gyros:	300°/sec FS;
Accelerometers:	5 G's FS
Magnetometers:	1.2 gauss FS
A/D Resolution:	16 bits
Nonlinearity	
Accelerometer:	0.2%
Gyro	0.2%
Magnetometer:	0.4%
Bias Stability	
Accelerometer:	0.010 G's
Gyro:	0.7°/sec
Magnetometer:	0.010 gauss
Orientation Resolution:	$<$ 0.1° minimum
Repeatability:	0.20°
Accuracy:	0.5° typical for static test conditions, 2° typical for dynamic test conditions and for arbitrary orientation angles
Output Modes:	Matrix, Quaternion, Euler angles and 9 scaled sensors with temperature
Digital Outputs:	Serial RS-232, RS-485 optional
Analog Output Option:	0-5 volts FS for Euler angles (pitch ±90°, roll ±180°, yaw ±180°)
Digital Output Rates:	100 Hz for Euler, Matrix, Quaternion 350 Hz for nine orthogonal sensors only
Serial Data Rate:	19.2/38.4/115.2 Kbaud, programmable
Supply Voltage:	5.2 VDC min, 12 VDC max
Supply Current:	65 milliamps
Connectors:	One keyed LEMO, two for RS-485
Operating Temperature:	-40° to +70° C with enclosure -40° to +85° C without enclosure
Size:	65×90×25 mm with enclosure 42×40×15 mm without enclosure
Weight:	74.6 g with enclosure 25.8 g without enclosure
Shock Limit:	1000 G's (unpowered) 500 G's (powered)

Table A.1: Microstrain 3DM-GX1 specifications [12].

A.2 GlobalSat EM–411

General	
Chipset:	SiRF StarIII
Frequency:	L1, 1575.42 MHz
C/A code:	1.023 MHz chip rate
Channels:	20 channel all-in-view tracking
Sensitivity:	-159 dBm
Position:	10 m, 2D RMS
	5 m, 2D RMS, WAAS enabled
Accuracy	
Velocity:	0.1 m/s
Time:	1μs synchronized to GPS time
Datum	
Default:	WGS-84
Acquisition Time	
Reacquisition:	0.1 s, average
Hot start :	1 s, average
Warm start:	38 s, average
Cold start:	42 s, average
Dynamic Conditions	
Altitude:	18,000 m max
Velocity:	515 m/s max
Acceleration:	Less than 4g
Jerk:	20m/sec^3
Power	
Main power input:	4.5V – 6.5V DC input
Power consumption:	60mA
Protocol	
Electrical level:	TTL level, Output voltage level:
	0V – 2.85V ,RS-232 level
Baud rate:	4,800 bps
Output message:	NMEA 0183
	GGA, GSA, GSV, RMC, VTG, GLL
Physical Characteristics	
Dimension:	30mm×30mm×10.5mm ± 0.3mm
Operating temperature:	-40° to +85°

Table A.2: GlobalSat EM–411 specifications [5].

Appendix B

Source Code

B.1 Matlab

B.1.1 gpsopen.m

```
%   name:           imuopen.m
%   Author:         Haakon Ellingsen
%   Created:        10/03-2008
%   Last modified:  21/05-2008
%   Description:    Opens the port for the GPS.
% Opening the serial port, the first command is
% platform/computer specific. For a stationary COM port on
% the windows platform, COM1 is usually correct. If in doubt,
% check the device manager. For linux systems, try e.g.
%'/dev/ttyCOM1' or '/dev/ttyUSB0'

fclose(instrfind)
s_gps = serial('COM13', 'baudrate', 4800);
fopen(s_gps);
```

B.1.2 gpsreader.m

```
i = 1;
text = fopen('gps.txt', 'w');
gpsTime = clock;
save gpsTime;
```

```
while(1)
    [data, n] = fscanf(s_gps);
    clear GPS;
    if(max(size(data))>6)
        GPS.name = data(2:6);
    else
        GPS.name = 0;
    end
    % Testing the data received
    if (max(find(data=='$')) ~= 1)
        GPS.name = 0;
    end
    % Only interested in the GPS data if GPRMC or GPGGA
    if(GPS.name == 'GPRMC')

        commas = find(data == ',');
        star = find(data == '*');
        if numel(commas)== 11
        GPS.time = data(commas(1)+1:commas(2)-1);
        GPS.status = data(commas(2)+1:commas(3)-1);
        GPS.lat =  data(commas(3)+1:commas(4)-1);
        GPS.NS = data(commas(4)+1:commas(5)-1);
        GPS.long = data(commas(5)+1:commas(6)-1);
        GPS.EW = data(commas(6)+1:commas(7)-1);
        GPS.SOG = data(commas(7)+1:commas(8)-1);
        GPS.COG = data(commas(8)+1:commas(9)-1);
        GPS.date = data(commas(9)+1:commas(10)-1);
        GPS.magVar = data(commas(10)+1:star(1)-1);
        GPS.chksm = data(star(1)+1:star(1)+2);
fprintf(text, '%s;%s;%s;%s;%s;%s;%s;\n',
    GPS.lat(1:2),GPS.lat(3:numel(GPS.lat)),
            GPS.long(1:2), GPS.long(3:numel(GPS.long)),
            GPS.SOG, GPS.COG, GPS.time);
        end
    elseif(GPS.name == 'GPGGA')
        commas = find(data == ',');
        star = find(data == '*');
                if numel(commas) == 14
        GPS.time = data(commas(1)+1:commas(2)-1);
        GPS.lat = data(commas(2)+1:commas(3)-1);
        GPS.NS =  data(commas(3)+1:commas(4)-1);
        GPS.long = data(commas(4)+1:commas(5)-1);
        GPS.EW = data(commas(5)+1:commas(6)-1);
        GPS.posFix = data(commas(6)+1:commas(7)-1);
        GPS.nSat = data(commas(7)+1:commas(8)-1);
        GPS.HDOP = data(commas(8)+1:commas(9)-1);
        GPS.h = data(commas(9)+1:commas(10)-1);
        GPS.AltUnit = data(commas(10)+1:commas(11)-1);
        GPS.GeoSep = data(commas(11)+1:commas(12)-1);
        GPS.GeoSepUnit = data(commas(12)+1:commas(13)-1);
        GPS.diffAge = data(commas(13)+1:commas(14)-1);
        GPS.diffRefId = data(commas(14)+1:star(1)-1);
        GPS.chksm = data(star(1)+1:star(1)+2);
 fprintf(text, '%s;%s%s%s;%s;%s;%s;\n',
            GPS.lat(1:2), GPS.lat(3:numel(GPS.lat)), GPS.long(1:2),
            GPS.long(3:numel(GPS.long)), GPS.h, GPS.posFix, GPS.time);
        end
    end
end
```

B.1.3 imuopen.m

```
%%%%%%%%%%%%%%%%%%%%%%%%%%%%%%%%%%%%%%%%%%%%%%%%%%%%%
%   name:           imuopen.m
%   Author:         Haakon Ellingsen
%   Created:        13/05-2008
%   Last modified:  16/05-2008
%   Description:    Opens a connection to the IMU

% Opening the serial port, the first command is
% platform/computer specific. For a stationary COM port on
% the windows platform, COM1 is usually correct. If in doubt,
% check the device manager. For linux systems, try e.g.
%'/dev/ttyCOM1' or '/dev/ttyUSB0'
s_imu = serial('COM13', 'baudrate', 115200,'DataBits',8);
fopen(s_imu);

% Creating and sending "enter continous mode" command to the IMU,
% meaning it will send data all the time.

% Is this wise in matlab, due to bad reading methods?
%cmd = hex2dec(['10';'00';'31'])';
%fwrite(s_imu,cmd,'uint8');
```

B.1.4 imureader.m

```
%   name:           imureader.m
%   Author:         Haakon Ellingsen
%   Created:        13/05-2008
%   Last modified:
%   Description:    Reads data from the IMU, and processes the data
%   received, making it

%cmd = hex2dec(['10'; '00'; '31'])';
cmd = hex2dec(['31']);
% Telling the IMU to write its data
fwrite(s_imu, cmd ,'uint8');
% Reading the IMU data

out = dec2hex(fread(s_imu, 23, 'uint8'));

% Processing the data
if(size(out) == [23 2])
    imu.header= hex2dec(out(1,:));
    imu.roll = hex2dec([out(2,:) out(3,:)]);
    imu.pitch = hex2dec([out(4,:) out(5,:)]);
    imu.yaw = hex2dec([out(6,:) out(7,:)]);
    imu.a_x = hex2dec([out(8,:) out(9,:)]);
    imu.a_y = hex2dec([out(10,:) out(11,:)]);
    imu.a_z = hex2dec([out(12,:) out(13,:)]);
    imu.omega_x = hex2dec([out(14,:) out(15,:)]);
    imu.omega_y = hex2dec([out(16,:) out(17,:)]);
    imu.omega_z = hex2dec([out(18,:) out(19,:)]);
    imu.timer = hex2dec([out(20,:) out(21,:)]);
    imu.chksm = [out(22,:) out(23,:)];

     % Calculating checksum
     calc_chksm = dec2hex(imu.header+imu.roll+imu.pitch
            +imu.yaw+imu.a_x+imu.a_y+imu.a_z+imu.omega_x
            +imu.omega_y+imu.omega_z+imu.timer);
     n_byt = size(calc_chksm);
     % Setting valid flag
     if (prev_time == Inf)
         imu_isValid = 0;
         prev_time = imu.timer;
         display('Can''t integrate without previous time. Run again')
     else
```

```
        imu_isValid = 1;
    end
else
    % Resetting valid flag
    imu_isValid = 0;
    display('Size received is wrong');
end
if imu_isValid
    if(imu.chksm == calc_chksm(n_byt(2)-3: n_byt(2)))
        % Means that the checksums matches, scaling the measurements
        imu.roll = imu.roll*g_gyro;
        imu.pitch = imu.pitch*g_gyro;
        imu.yaw = imu.yaw*g_gyro;
        if(imu.a_x>32768) % Overflow, meaning negative number.
            imu.a_x = (imu.a_x-65536)*g_acc;
        else
            imu.a_x = imu.a_x*g_acc;
        end
        if(imu.a_y>32768) % Overflow, meaning negative number.
            imu.a_y = (imu.a_y-65536)*g_acc;
        else
            imu.a_y = imu.a_y*g_acc;
        end
        if(imu.a_z>32768) % Overflow, meaning negative number, correcting
            imu.a_z = (imu.a_z-65536)*g_acc;
        else
            imu.a_z = imu.a_z*g_acc;
        end
        if(imu.omega_x>32768) % Overflow, meaning negative number.
            imu.omega_x = (imu.omega_x-65536)*g_rate;
        else
            imu.omega_x = imu.omega_x*g_rate;
        end
        if(imu.omega_y>32768) % Overflow, meaning negative number.
            imu.omega_y = (imu.omega_y-65536)*g_rate;
        else
            imu.omega_y = imu.omega_y*g_rate;
        end
        if(imu.omega_z>32768) % Overflow, meaning negative number.
            imu.omega_z = (imu.omega_z-65536)*g_rate;
        else
            imu.omega_z = imu.omega_z*g_rate;
        end
```

```
            imu_isValid = 1;
        else
            % Means that the two checksums are different, rejecting the data
            imu_isValid = 0;
            display('Checksum calculation failed')
        end
    end
    if imu_isValid
        % Evaluating the timer
        delta_t = imu.timer-prev_time;
        if (delta_t < 0)
            delta_t = delta_t + 65536;
        end
        prev_time = imu.timer;
        % The rollover is accounted for, scaling the measurement
        delta_t = delta_t * 0.0065536;
        fprintf(text, '%i;%i;%i;%i;%i;%i;%i\n', imu.a_x, imu.a_y,
               imu.a_z, imu.roll, imu.pitch, imu.yaw, delta_t);
    end
%     % Updating the rotation matrix
%     Rb2n = updateR(imu.roll, imu.pitch, imu.yaw);
%     % Solving the differential equation
%     prev_imu = imu;
%     imu.a = Rb2n*([imu.a_x; imu.a_y; imu.a_z]-bias)+[0; 0; g_const]+
%[boat.v(2)*2*omega_ie*sind(boat.long);
%boat.v(1)*2*omega_ie*sind(boat.long)
%+boat.v(3)*2*omega_ie*cosd(boat.long);
%-boat.v(2)*2*omega_ie*cosd(boat.long)];
%     imu.v = imu.v + imu.a*delta_t;
%     imu.p = imu.p + imu.v*delta_t;
%  figure(1)
%      plot([prev_imu.p(2);imu.p(2)], [prev_imu.p(1);imu.p(1)]);
%      drawnow();

% %  figure(2)
% %  % Euler angles
% %  for i = 1:3
% %      if i == 1
% %         hold off;
% %         plot3([0;Rb2n(i,1)],[0;Rb2n(i,2)],[0;Rb2n(i,3)]);
% %         hold on;
% %         grid on
% %      end
% %       plot3([0;Rb2n(i,1)],[0;Rb2n(i,2)],[0;Rb2n(i,3)]);
% %       axis([-1,1,-1,1,-1,1]);
% %   end
%
% figure(3)
% % Acceleration
% total_t = total_t + delta_t;
% for i = 1:3
%     subplot(3,1,i)
%         plot([total_t-delta_t;total_t],[prev_imu.a(i), imu.a(i)]);
%         plot([total_t-delta_t;total_t],[prev_bias(i),bias(i)],'r--')
%         plot([total_t-30, total_t],[0 0],'b')
%         axis([total_t-30, total_t, -5, 5])
%         ylim('auto')
% end
% prev_bias = bias;
% drawnow();
% GPS.time = GPS.time+delta_t;
% end
%
%
%
%
```

B.1.5 IMU_f.m

```
function ret = IMU_f(x, u, a, e)
  R_phi = a*(1-e^2)/(1-(e*sin(x(1,1))^2)^1.5);
  R_lambda = a/sqrt(1-(e*sin(x(1,1))^2));
  omega_ie = 7.292115E-5;
% x = [phi, lambda, h, v_n, v_e, v_d]
  out(1, 1) = 1 / (R_phi + x(3,1)) * x(4,1);                    % dPhi/dt
  out(2, 1) = 1 / (R_lambda + x(3,1)) * cos(x(1,1)) * x(5,1); % dlambda/dt
  out(3, 1) = -x(6,1);                                           % dh/dt
  out(4, 1) = u(1,1) - (out(1,1) + 2 * omega_ie) * sin(x(2,1))
            * x(5,1) + out(2,1) * x(3,1);
  out(5, 1) = u(2,1) + (out(1,1) + 2 * omega_ie) * sin(x(2,1))
            * x(4,1) + (out(1,1) + 2 * omega_ie) * cos(x(2,1)) * x(6,1);
  out(6, 1) = u(3,1) - (out(1,1) + 2 * omega_ie) * cos(x(2,1))
            * x(5,1) + out(2,1) * x(1,1);
  ret = out;
```

B.1.6 sysinit.m

```
clear all;
close all;
global omega_ie;
global Q;
global R;

lat = 10+32/60+20/60/60;
long = 63+25/60+46/60/60;
text = fopen('imu.txt', 'w');
total_t = 0;
prev_bias = [0, 0, 0]';
R = diag([5*ones(1,3), ones(1,3)]);
Q = eye(9);
omega_ie = 7292115e-11;
I3 = eye(3);
O3 = zeros(3,3);
A = [O3 I3 O3;
    O3 O3 I3
    O3 O3 O3];
%B = [O3; I3];
D = [O3 O3; I3 O3; O3 I3];
C = [I3 O3 O3];
bias = zeros(3,1);
% Calculating gravity
lambda = 63.36;
gamma_a = 9.78049;
f = 1/298.257223563;
m = 0.00344978650684;
f_2 = -f+5/2*m+1/2*f^2-26/7*f*m+15/4*m^2;
f_4 = -1/2*f^2+5/2*f*m;
g_const = gamma_a*(1+(f_2+f_4)*sind(lambda)^2-1/4*f_4*sind(2*lambda)^2);
% This is the gravity calculated using the gravity model


% Flag to denote that imu measurement passes all tests
imu_isValid = 0;
prev_time = Inf;

fclose(instrfind)
delete(instrfind)
imuopen;
```

```
% Defining gain constants for accelerometer and gyro.
g_acc = 9.81*7000/32768000;
g_gyro = 360/65536;
g_rate = 8500/32768000;
%cmd = hex2dec(['10'; '00'; '31'])';
% Telling the IMU to write its data
%fwrite(s_imu, cmd ,'uint8');
%out = fread(s_imu, 7, 'uint8');
while(1)
    imureader;
end
```

B.1.7 kalman.m

```
function [bias, P] = KalmanFilter(kalm_y, P, Rt2E, dt)
    kalm_I = eye(9);
    kalm_Q = [zeros(3,9);
              zeros(3,3) 0.025*eye(3) zeros(3,3);
              zeros(3,6) 0.1*eye(3)];
    kalm_R = [eye(3)*1E-10 zeros(3,3);
             zeros(3,3) 1*eye(3)];
    kalm_A = -eye(9);
    kalm_A(1,4) = Rt2E(1)*dt;
    kalm_A(2,5) = Rt2E(2)*dt;
kalm_A(3,6) = Rt2E(3)*dt;
kalm_A(4,7) = -dt;
    kalm_A(5,8) = -dt;
    kalm_A(6,9) = -dt;

kalm_C = [eye(3), zeros(3,6);
              zeros(3,3) eye(3) zeros(3,3)];
P_pre = kalm_A*P*kalm_A'+kalm_Q;
kalm_K = P_pre*kalm_C'*inv(kalm_C*P_pre*kalm_C'+kalm_R);
P = (kalm_I-kalm_K*kalm_C)*P_pre;
x = kalm_K*kalm_y;
bias = x;
```

B.1.8 proc.m

```
clear all;
```

```
close all;
count = 1;
load imu.txt
load gps.txt
id_gps = false;

posoffs = [0.10, 0, 0]';
numit = 0;
totatt = [0 0 0]';
%count = 1;
count2 = 0;
roll = imu(:,4);
pitch = imu(:,5);
yaw = imu(:,6)-90;
a.x = imu(:,1);
a.y = imu(:,2);
a.z = -imu(:,3);

gps_data.lat = (gps(:,1)+gps(:,2)/60)*pi/180;
gps_data.long = (gps(:,3)+gps(:,4)/60)*pi/180;
gps_data.SOG = gps(:,5);
gps_data.COG = gps(:,6);
gps_data.time = gps(:,7);
gps_data.time(1:39) = gps_data.time(1:39)+40;
startTime = gps_data.time(1);

% for i = 1:numel(mat(:,1))
%     mat(i,:) = mat(i,:)*(diag(1.2-0.4*rand(1,3)));
%
% end
% a.x = mat(:,1)+a.x(1:numel(mat(:,1)));
% a.y = mat(:,2)+a.y(1:numel(mat(:,1)));
% a.z = mat(:,3)+a.z(1:numel(mat(:,1)));
dt = imu(:,7);

WGS_a = 6378137;
WGS_e = 0.08181979099211;
x = [gps_data.lat(1) gps_data.long(1) 0 0 0 0]';

prevAccel = [0, 0, 0]';
totalTime = 0;
biasAcc = [-0.2 0.5 0]';
%biasAcc = [0 0 0]';
```

```
P=eye(9);
alltime = 0;
prevtime = 0;
prevX = x;
figure(1);
subplot(3,1,1)
hold on;
xlabel('Time [s]')
ylabel('Pos N [m]')
subplot(3,1,2)
hold on;
legend('\Phi', '\lambda', 'h')
xlabel('Time [s]')
ylabel('Pos E [m]')
subplot(3,1,3)
hold on;
legend('\Phi', '\lambda', 'h')
xlabel('Time [s]')
ylabel('Pos D [m]')
figure(2);
hold on;
figure(3)
hold on;
legend('a_x', 'a_y', 'a_z')
    start = x;
for i = 1:size(a.x)

    prevX = x;
dt(i) = 0.1;
    prevtime = alltime;
    Rb2t = updateR(roll(i), pitch(i), yaw(i));

    accel = Rb2t*([a.x(i), a.y(i), a.z(i)]'+biasAcc)-[0 0 9.9506]';

    c1 = 0.5;
c2 = 0.5;
c3 = 1.0;
b1= 1/6;
b4 = 1/6;
b2 = 1/3;
b3 = 1/3;
a21 = 0.5;
a32 = 0.5;
```

```
a43 = 1.0;
    k1 = IMU_f(x, prevAccel, WGS_a, WGS_e);
    k2 = IMU_f(x+dt(i)*a21*k1,(1-c1)*prevAccel+c1*accel, WGS_a, WGS_e);
    k3 = IMU_f(x+dt(i)*a32*k2, (1-c2)*prevAccel+c2*accel, WGS_a, WGS_e);
    k4 = IMU_f(x+dt(i)*a43*k3,(1-c3)*prevAccel+c3*accel, WGS_a, WGS_e);
x = x + dt(i)*(b1*k1+b2*k2+b3*k3+b4*k4);
    prevAccel = accel;
    totalTime = totalTime + dt(i);
    alltime = alltime +dt(i);

    totatt = totatt + [roll(i), pitch(i), yaw(i)]';
    numit = numit +1;
%if false
    if count <= numel(gps_data.time)
     if totalTime >= gps_data.time(count)-gps_data.time(1)
         % && (count < 40 || totalTime > 60)
         count2 = count2 +1;
         if totalTime>60 && count < 50
             count = 60;
         end

         R_phi = WGS_a*(1-WGS_e^2)/(1-(WGS_e*sin(x(1,1)))^2)^1.5;
         R_lambda = WGS_a/sqrt(1-(WGS_e*sin(x(1,1)))^2);
         Rt2E = [1/(R_phi+x(3,1)); 1/(R_lambda+x(3,1))/cos(x(1,1)); -1];
        % Transferring the offset to ECEF
         tmpoff = diag(Rt2E)*Rb2t*posoffs;
         % Only used for calculating RMS values
         gps_speed = gps_data.SOG(count)*[cosd(gps_data.COG(count))
                                          sind(gps_data.COG(count))
                                          0];
         tmp(count,:) = gps_speed-x(4:6)';
         x_tilde = [gps_data.lat(count)
                   , gps_data.long(count)
                    , 0, gps_speed]'-[tmpoff; 0; 0; 0] - x;
        if id_gps
            % Using ideal gps, test purposes only
            gps_speed = gps_speed*0;
            x_tilde = [gps_data.lat(1), gps_data.long(1), 0, gps_speed]'-x;
        end
        est_s(count, :) = [gps_speed, gps_data.time(count)];
        if count2 >10
            P = eye(9);
            count2 = 0;
        end
        [bias, P] = kalman(x_tilde, P, Rt2E, totalTime);
        x = x + bias(1:6);
        if numit < 50
         Rb2t = updateR(totatt(1)/numit, totatt(2)/numit, totatt(3)/numit);
        else
            x(1:3) = [gps_data.lat(count), gps_data.long(count), 0]';
        end
        biasAcc = biasAcc + inv(Rb2t)*bias(7:9);
        biascount(count, :) = biasAcc;
        gpspos(count,:) = [(gps_data.lat(count)-gps_data.lat(1))/Rt2E(1),
                           (gps_data.long(count)-gps_data.long(1))/Rt2E(2),
                           0];
        count = count + 1;
        totatt = [0 0 0]';
        numit = 0;
%        x(3) = 0;
     end
    else
        break
    end
%end
accel2(i,:) = ([a.x(i), a.y(i), a.z(i)]'+biasAcc)-inv(Rb2t)*[0 0 9.9506]';

  R_phi = WGS_a*(1-WGS_e^2)/(1-(WGS_e*sin(x(1,1)))^2)^1.5;
  R_lambda = WGS_a/sqrt(1-(WGS_e*sin(x(1,1)))^2);
  data(i,:) = [totalTime, (R_phi+x(3,1))*(x(1)-gps_data.lat(1))
                      (R_lambda+x(3,1))*cos(x(1,1))*(x(2)-gps_data.long(1))
                      -x(3), x(4:6)', accel'];
end
    figure(1)
    subplot(3,1,1)
       hold on;
       plot(data(:,1), data(:,2));
       plot(gps_data.time(1:numel(gpspos(:,3)))-gps_data.time(1),
                gpspos(:,1), '--r')
       legend('Estimated','GPS');
       % plot(0:70,0, '--b')
       axis([0 55 -1 1])
       axis 'auto y';
    subplot(3,1,2)
        hold on;
        plot(data(:,1), data(:,3));
        plot(gps_data.time(1:numel(gpspos(:,3)))-gps_data.time(1),
                gpspos(:,2), '--r')
        legend('Estimated','GPS');
       % plot(0:70,0, '--b')
        axis([0 55 -1 1])
       axis 'auto y';
    subplot(3,1,3)
        hold on;
        plot(data(:,1), data(:,4));
        plot(gps_data.time(1:numel(gpspos(:,3)))-gps_data.time(1),
                gpspos(:,3), '--r')
        legend('Estimated','GPS');
        axis([0 55 -1 1])
        axis 'auto y';
    figure(2)
    subplot(3,1,1)
        hold on;
     %   plot(0:70,0, '--b')
        plot(data(:,1), data(:,5));
        xlabel('Time [s]')
        ylabel('Speed N [m/s]')
       axis([0 55 -1 1])
        axis 'auto y';
    subplot(3,1,2)
        hold on;
     %   plot(0:70,0, '--b')
        plot(data(:,1), data(:,6));
        xlabel('Time [s]')
        ylabel('Speed E [m/s]')
        axis([0 55 -10 25])
%        axis 'auto y';
    subplot(3,1,3)
        hold on;
    %    plot(0:70,0, '--b')
        plot(data(:,1), data(:,7));
        xlabel('Time [s]')
        ylabel('Speed D [m/s]')
        axis([0 55 -1 2])
        axis 'auto y';
    figure(3)
    subplot(3,1,1)
        hold on;
     %   plot(0:70,0, '--b')
```

```
        plot(data(:,1), accel2(:,1));
        xlabel('Time [s]')
        ylabel('Acc x [m/s^2]')
        axis([0 55 -1 1])
        axis 'auto y';
    subplot(3,1,2)
        hold on;
    %    plot(0:70,0, '--b')
        plot(data(:,1), accel2(:,2));
        xlabel('Time [s]')
        ylabel('Acc y [m/s^2]')
        axis([0 55 -1 1])
        axis 'auto y';
    subplot(3,1,3)
        hold on;
   %     plot(0:70,0, '--b')
        plot(data(:,1), accel2(:,3));
        xlabel('Time [s]')
        ylabel('Acc z [m/s^2]')
        axis([0 55 -1 1])
        axis 'auto y';
figure(4);
subplot(311)
plot(est_s(:,4)-est_s(1,4), est_s(:,1))
subplot(312)
plot(est_s(:,4)-est_s(1,4), est_s(:,2))
subplot(313)
plot(est_s(:,4)-est_s(1,4), est_s(:,3))

start = 35;
% Calculating RMS values
p_n = sqrt(data(start:numel(data(:,2)),2)'*data(start:numel(data(:,2)),2)/
        (numel(data(:,2))-start+1));
p_e = sqrt(data(start:numel(data(:,3)),3)'*data(start:numel(data(:,3)),3)/
        (numel(data(:,3))-start+1));
p_d = sqrt(data(start:numel(data(:,4)),4)'*data(start:numel(data(:,4)),4)/
        (numel(data(:,4))-start+1));
v_n = sqrt(data(start:numel(data(:,5)),5)'*data(start:numel(data(:,5)),5)/
        (numel(data(:,5))-start+1));
v_e = sqrt(data(start:numel(data(:,6)),6)'*data(start:numel(data(:,6)),6)/
        (numel(data(:,6))-start+1));
v_d = sqrt(data(start:numel(data(:,7)),7)'*data(start:numel(data(:,7)),7)/
        (numel(data(:,7))-start+1));
```

```
a_x = sqrt(accel2(:,1)'*accel2(:,1)/numel(accel2(:,1)));
a_y = sqrt(accel2(:,2)'*accel2(:,2)/numel(accel2(:,2)));
a_z = sqrt(accel2(:,3)'*accel2(:,3)/numel(accel2(:,3)));

figure(5);
plot(biascount)
legend('X', 'Y', 'Z')
xlabel('Time [s]')
ylabel('Bias [m/s^2]'
```

B.1.9 Rt2eg.m

```
function [R] = Rt2eg(Phi, lambda, h)
    a = 6378137;
    e = 8.1819190842622E-2;
    R_phi = a*(1-e^2)/sqrt(1-e^2*sind(Phi)^2);
    R_lambda = a/sqrt(1-e^2*sind(Phi)^2);
    R = [1/(R_phi+h) 0 0;
        0 1/((R_lambda+h)*cosd(lambda)) 0;
        0 0 -1];
```

B.1.10 sysinit.m

```
clear all;
close all;
global omega_ie;
global Q;
global R;

lat = 10+32/60+20/60/60;
long = 63+25/60+46/60/60;
text = fopen('imu.txt', 'w');
total_t = 0;
prev_bias = [0, 0, 0]';
R = diag([5*ones(1,3), ones(1,3)]);
Q = eye(9);
omega_ie = 7292115e-11;
I3 = eye(3);
O3 = zeros(3,3);
A = [O3 I3 O3;
    O3 O3 I3
    O3 O3 O3];
%B = [O3; I3];
D = [O3 O3; I3 O3; O3 I3];
C = [I3 O3 O3];
bias = zeros(3,1);
% Calculating gravity
lambda = 63.36;
gamma_a = 9.78049;
f = 1/298.257223563;
m = 0.00344978650684;
f_2 = -f+5/2*m+1/2*f^2-26/7*f*m+15/4*m^2;
f_4 = -1/2*f^2+5/2*f*m;
g_const = gamma_a*(1+(f_2+f_4)*sind(lambda)^2-1/4*f_4*sind(2*lambda)^2);
% This is the gravity calculated using the gravity model


% Flag to denote that imu measurement passes all tests
imu_isValid = 0;
prev_time = Inf;

fclose(instrfind)
delete(instrfind)
imuopen;

% Defining gain constants for accelerometer and gyro.
g_acc = 9.81*7000/32768000;
g_gyro = 360/65536;
g_rate = 8500/32768000;
%cmd = hex2dec(['10'; '00'; '31'])';
% Telling the IMU to write its data
%fwrite(s_imu, cmd ,'uint8');
%out = fread(s_imu, 7, 'uint8');
while(1)
    imureader;
end
```

B.1.11 updateR.m

```
function [Rb2t] = updateR(phi, theta, psi)
    Rb2t = [cosd(psi)*cosd(theta)
           -sind(psi)*cosd(phi)+cosd(psi)*sind(theta)*sind(phi)
            sind(psi)*sind(phi)+cosd(psi)*sind(theta)*cosd(phi);
sind(psi)*cosd(theta)
cosd(psi)*cosd(phi)+sind(psi)*sind(theta)*sind(phi)
 -cosd(psi)*sind(phi)+sind(psi)*sind(theta)*cosd(phi);
-sind(theta)
cosd(theta)*sind(phi)
cosd(theta)*cosd(phi)];
```

Bibliography

[1] Volker Bertram. Unmanned surface vehicles – a survey. Technical report, ENSIETA, 2008.

[2] K. Betke. The NMEA 0183 protocol. Technical report, 2001.

[3] M. Brain. http://www.howstuffworks.com (picture only).

[4] A. K. Brown and Y. Lu. Performance test results of an integrated GPS/MEMS inertial navigation package. *ION GNSS*, 2004.

[5] GlobalSat Technology Corporation. Product user manual, GPS receiver engine board EM–411. http://www.globalsat.com.tw, accessed on 10/5-2008.

[6] J. Doe. http://www.mistupid.com (picture only).

[7] C. Dubay and T. Johns. WAAS, DGPS and the Mariner's Toolkit. Technical report, US Coast Guard, 2000.

[8] M. K. Eriksen. Ground station and hardware peripherals for fixed-wing UAV: Cyberswan. Master's thesis, Norwegian University of Science and Technology, 2007.

[9] J. A. Farrell and M. Barth. *The Global Positioning System & Inertial Navigation*. R. R. Donnelley & Sons Company, 1999.

[10] R. Henriksen. Stokastiske systemer, 1998.

[11] O. C. Jakobsen. Low cost integrated navigation systems. Master's thesis, Norwegian University of Science and Technology, 2004.

[12] Microstrain. 3DM–GX1 gyro enhanced orientation sensor. http://www.microstrain.com, accessed on 10/5-2008.

[13] C. Pellerin. United states updates global positioning system technology. Technical report, www.america.gov, 2006, accessed on 8/3-2008.

[14] G. Pendleton. http://www.directionsmag.com (picture only), 2002.

[15] The World Geodetic System. Its definition and relationships with local geodetic systems. Technical report, The United States Department Of Defense, 1984.